Applications of Smart Materials in Structural Engineering

by

C. S. Cai, Ph.D., P.E.
Wenjie Wu
Suren Chen
George Voyiadjis, Ph.D.

Department of Civil Engineering
Louisiana State University
Baton Rouge, Louisiana 70803

LTRC Project No. 02-4TIRE
State Project No. 736-99-1055

Conducted for

Louisiana Department of Transportation and Development
Louisiana Transportation Research Center

October 2003

ABSTRACT

With the development of materials and technology, many new materials find their applications in civil engineering to deal with the deteriorating infrastructure. Smart material is a promising example that deserves a wide focus, from research to application. With two crystal structures called Austenite and Martensite under different temperatures, smart material exhibits two special properties different from ordinary steels. One is shape memory, and the other is superelasticity. Both of these two properties can suit varied applications in civil engineering, such as prestress bars, self-rehabilitation, and two-way actuators, etc.

One of the main objectives of the research is to investigate the application of smart materials in civil engineering by focusing on the literature review, basic information collection, and basic mechanic properties of smart materials. In axial tension tests, the force-extension curve and stress-strain curve of shape memory and superelasticity materials were measured separately. These curves verify the research of forerunners.

Four beam experiments were conducted to evaluate the performance of flexure beams with superelasticity material as reinforcement bars. Load-displacement relationship at the mid-span, strains on the surface of the concrete beam, and cracking width for different loads were measured.

This research is just the first step in the investigation of the application of smart materials in structural engineering. Some bigger beams are prepared for experiments in the near future.

ACKNOWLEDGMENTS

The investigators appreciate the Louisiana Transportation Research Center (LTRC) for funding this project through the Transportation Innovation for Research Exploration (TIRE) Program.

The investigators also want to express their thanks to those who provided help during the development of the research program.

Walid Alaywan, Project Manager, LTRC

Randy Young, Senior Concrete Technician, LTRC

Alvin Mix, III, Concrete Technician, LTRC

Matt Tircuit, Concrete Technician, LTRC

Sadi Torres, Research Engineer, LTRC

Khiet Ngo, Material Lab, DOTD of Louisiana

Al Pawlowski, Technician, Civil Engineering, Louisiana State University

The investigators also want to express their thanks to the following individuals and companies who provide information and materials to this project:

Subhash Gupta, Product Engineer, Special Metals Corporation

K. Mio, Sales Manager, Awaji Sangyo Corporation

Dave Niedermaier, Nitinol Device and Components

IMPLEMENTATION STATEMENT

The purpose of the TIRE program is not to perform research for immediate implementation. Instead, it provides seed money to explore new areas related to transportation systems and eventually develops larger-scale research proposals for federally funded research projects, if the research is promising. If the research is not feasible, TIRE provides an opportunity to document why further investment is not warranted.

Once technical difficulties are overcome, one potential application is to use smart materials (superelasticity property) as self-repair materials in bridges and pavements. One can also use smart material strands (shape memory property) as additional prestressing strands that are used on as-needed basis to counterbalance excessive prestress losses, or even allow the structure to gain additional capacity in the case of overweight trucks. In major bridge applications, wireless /remote techniques can be used to monitor and control the bridges by activating the smart strands. Some of the features of these smart materials can also be self-activated.

However, many technical difficulties, cost issues, and design issues need to be resolved before smart materials can actually be applied on a large-scale to civil engineering structures.

TABLE OF CONTENTS

LIST OF TABLES

LIST OF FIGURES

INTRODUCTION

Concept of Smart Materials

With the development of material science, many new, high-quality, and cost-efficient materials have come into use in structural engineering. Smart material is one good example. Since Nickel-Titanium smart material was first studied in Naval Ordinance Laboratory *[1]*, it rapidly found applications in many fields such as aerospace, mechanical and biomedical engineering etc. Today, more and more researchers are focusing on smart materials for their special properties and performance in civil engineering applications.

Smart material can exist in two phases at different temperatures: Austenite, which exists in high temperature, and Martensite, which exists in low temperature. When the external temperature or stress condition changes, these two phases will transform to the other phase, depending on what change appears. Smart material exhibits many special properties during the transformations between these two phases, such as shape memory effect, superelasticity effect, and two-way memory effect, etc.

Perhaps, the most vivid show of the potential of shape memory alloy has been the television commercial in which a pair of eyeglasses is twisted around someone's finger. The moment the person releases them, the eyeglasses snap back into their proper shape. This is known as superelasticity. It is actually the shape memory property of Shape Memory Alloys (SMA) that allows them to do so. As the wire is bent, the increased stress causes the wire to transform from Austenite to Martensite phase. However, when the wire is released, the stress drops to zero and the wire shifts back to the Austenite phase and its original shape.

The field of smart materials and structures is emerging rapidly with technological innovations in engineering materials, sensors, actuators and image processing. Smartness describes self-adaptability, self-sensing, memory, and multiple functionalities of the materials or structures. These characteristics provide numerous possible applications for these materials and structures in aerospace, manufacturing, civil infrastructure systems, and biomechanics. Self-adaptation characteristics of smart structures are a great benefit that utilizes the embedded adaptation of smart materials like shape memory alloys. By changing their properties, smart materials can detect faults and cracks and therefore are useful as a diagnostic tool. This characteristic can be utilized to activate the smart material embedded in the host material in a proper way to compensate for the fault. This phenomenon is called self-repairing effect.

Shape Memory Alloy (SMA) is a special class of adaptive material that can convert thermal energy directly into mechanical work. When properly mixed, a variety of alloys exhibit this effect by repeated heat treatments. Shape memory effect in various alloys has been documented since the early 1930s, leading to a number of commercial products in the mechanical and aerospace industries. Ni-Ti is the most commonly used SMA *[2]*.

When SMA is subjected to plastic deformation at low temperatures $T < A_s$, (where A_s = Austenite start temperature), it undergoes a mechanical twining process in which each adjacent layer of atoms moves by one lattice parameter. However, when the material is heated above A_f, (where A_f = Austenite finish temperature), it undergoes a phase transformation, recovering most of the mechanically imposed deformation and restoring to the original "memory" shape of the specimen. This effect is referred to as one-way memory effect. Through special heat treatment process, two-way memory effect can be achieved. The two-way memory alloys can undergo large and opposite deformations upon heating and cooling and can serve as two-way actuators. That is, heating the SMA results in one memorized shape while cooling results in a second different shape. Using this two-way effect, the SMA can expand or shrink so that it can apply and remove stress in a structure on an as-needed basis, which can lead to a smart structure.

The phase transformation temperatures depend on not only the material composition, but also the stress state. When stress changes, the phase transformation temperatures may also change. This means that the phase transformation can also be activated without actual temperature change, but through a stress change, as is the case demonstrated by the eyeglass example discussed above. This property provides a promising application in self-repair. When concrete structures start to crack, the increased stress in the SMA may activate the phase transformation, which produces compressive stress in the structures to limit the cracking. Another important property of SMA is that temperature increases may result in shrinkage due to phase transformation. This shrinkage may also be utilized to balance the thermal expansion. Therefore, SMA may be a very promising material to deal with temperature induced stress/cracking problems.

Problems in Highways and Bridges

Differential settlement between bridges and pavements causes bumps or uneven joints at the bridge ends. When vehicles, especially heavy trucks, approach and leave bridges, the bumps cause large impact loads to the bridges and pavements. It is well known that these uneven joints can cause pavement and bridge deterioration, damage automobiles or cause accidents. The damage includes separation of pavement topping from its base, spalling of

joints, fatigue cracking of pavements, and fatigue damage to bridges. A similar problem is associated with the uneven settlement between the piers of the bridge or the approach spans. When differential settlement occurs, not only is the drivability of the bridge affected, but additional internal forces are also created for the structure. Maintenance of joints is a big problem and expense for engineers and highway officials. Traditionally, in dealing with these problems, engineers focus on improvement in foundation design. However, they have not been very successful in resolving these problems associated with the unevenness of the joints and differential settlement.

Temperature change and time-dependent effects, such as creep and shrinkage, also cause internal restraint forces for indeterminate structures. These forces alone or together with other external load effects cause cracking of existing structures and pavements, or increase the cost for new construction meant to cope with these effects (such as increase in section dimensions).

Another problem is that associated with the performance of bridge bearing. Malfunctioning bearings due to material deterioration, clogging of dirt, and other factors result in tremendous stresses near the bearing region. This causes changes in the force redistribution and thus makes the bridges behave differently from the intended design. These problems are common factors in bridge failures and in maintenance requirements. Finding a way to automatically adjust forces among the bearings in order to alleviate all of the above problems is desirable.

Concept of Smart Bridges

The two-way memory effects of SMA can be used to make SMA actuators that can rise and fall to adjust their heights. The SMA can also be used to manufacture smart strands. After mechanically deforming the strands and embedding them in concrete, the prestressing and self-repair effects can be activated as needed during the life of the structure. The smart strands are actually actuators that can be activated by external heating or internal stress changes.

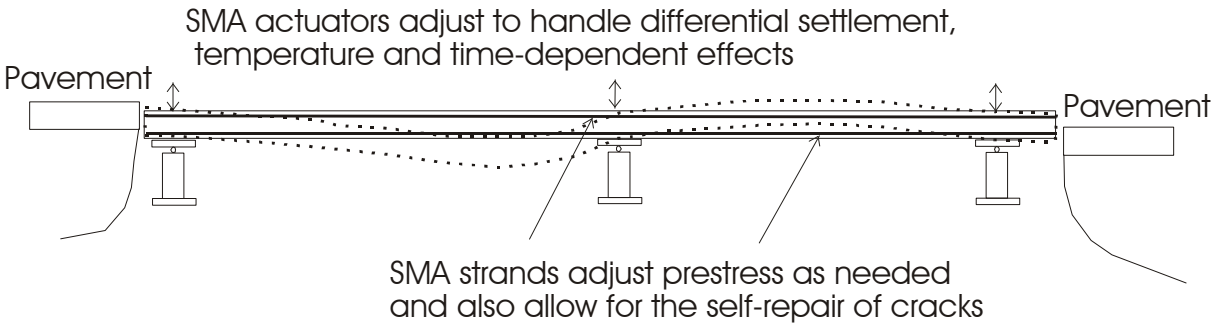

Figure 1 Sketch of a smart bridge

The applications of the smart bearings and smart strands can be used to develop a smart bridge as shown in figure 1. The smart bearings will adjust their heights through the shape memory effect of the SMA. This height adjustment will correct the unevenness problem as well as the internal forces induced from differential settlements, time-dependent deformations (creep and shrinkage of concrete, relaxation of prestressing steel), and temperature changes as discussed earlier. When needed, the prestress forces can also be adjusted to deal with cracking issues in both positive and negative moment zones. With the combined application of the smart bearings and smart strands, the bridge can adjust its internal force distribution and mobilize each element to adapt itself to different environmental loads like those induced by differential settlement, time-dependent effects, temperature effects, and over-weight trucks.

The purpose of the present study is to collect background information, explore possibilities, and lay a foundation for further research in developing a smart bridge system.

OBJECTIVE

This research focuses on exploring possible applications of smart materials in civil engineering by reviewing and collecting related literature, accumulating basic first-hand knowledge about the smart material itself, and developing a basic structural element with smart materials. Material property tests and simply supported beam experiments were performed to obtain needed information about the parameters of the materials used in this research and to verify the potential applications of smart materials in structural engineering, such as the self-rehabilitation of the cracking of concrete members.

The results of this research will serve as a seed that will initiate more research in this area. Based on this research, additional research investigating prestress effect, self-repair capability, and two-way memory training can be performed in the future, which will eventually lead to the development of a smart bridge system.

SCOPE

This research is divided into the following sub-tasks.

Task 1: Literature Review and Information Collection

Necessary literature review and collection of information regarding available smart material products was conducted to select the most appropriate material for this research. Different smart materials were compared in terms of phase transformation temperature, material properties, price range, etc., before the most appropriate one was chosen.

Task 2: Material Tests

a. Force-extension and stress-strain curve of superelasticity material.

b. Force-extension and stress-strain curve of shape memory material.

Task 3: Beam Experiments

a. Force-displacement curve at the mid-span, force-cracking width curve at certain loading steps and force-strain curve at different points of concrete beams with superelasticity smart material.

b. Cracking self-rehabilitation of concrete beams with superelasticity smart material.

METHODOLOGY

Literature Review

A relatively new material, smart material has been extensively studied in recent years in aerospace, mechanical, and biomedical applications. Based on these research results, a few applications have been tested in civil engineering laboratory experimental and field practice.

History of Smart Materials

The first recorded observation of smart material transformation was made in 1932 on gold-cadmium. In addition, in 1938 the phase transformation was observed in brass (copper-zinc). It was not until 1962, however, that Beehler and coworkers found the transformation and attendant shape memory effect in Nickel-Titanium at the Naval Ordinance Laboratory. They named this family of alloy Nitinol after their lab. A few years after the discovery of Nitinol, a number of other alloy systems with the shape memory effect were found *[1]*.

Though product development using smart materials began to accelerate after the discovery of Nitinol, many of the smart materials contained expensive and exotic elements. Only the copper-based alloys came close to challenging the Nitinol family as a commercially attractive system. During the 1980s and early 1990s, a number of companies began to provide Ni-Ti materials and components, and an increasing number of products, especially medical products, were developed to market *[1], [3]*.

Transformation Mechanism of Smart Material

Smart materials exist as two stable phases under different temperatures: Austenite, the high-temperature phase, and Martensite, the low-temperature phase. In addition, there are two different forms of Martensite materials: twinned and detwinned (figure 2). At a certain temperature, smart material will stay at its thermodynamically stable phase. However, when temperature changes, transformations between these two phases occur. Due to this transformation mechanism, smart materials have many special properties, such as shape memory effect and superelasticity effect that have a wide potential use in structural applications.

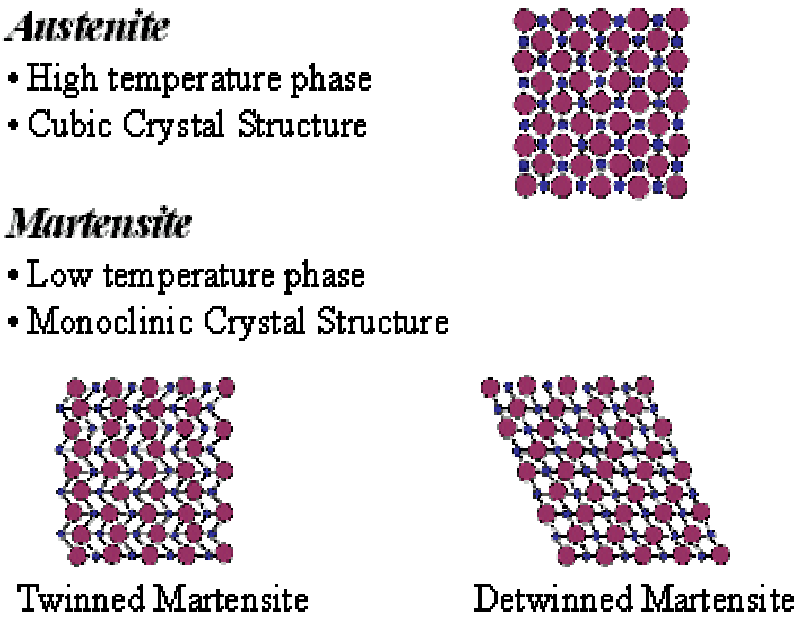

Figure 2
Different phases of smart materials (Smart Lab at TAMU) *[4]*

Shape memory is one of those special properties. When the smart material in twinned Martensite phase undergoes external stress, it transforms to detwinned Martensite phase as Procedure 1 indicates (figure 3). There is no temperature change during this transformation. When the detwinned Martensite material undergoes an increase in temperature, the detwinned Martensite transforms to Austenite as seen in Procedure 2. As Procedure 3 indicates, Austenite will go back to twinned Martensite when the temperature goes down. There are four characteristic temperature points between Procedures 2 and 3, in the ascending temperature sort:

M_f, Martensitic finish temperature;
M_s, Martensitic start temperature;
A_s, Austenite start temperature; and
A_f, Austenite finish temperature.

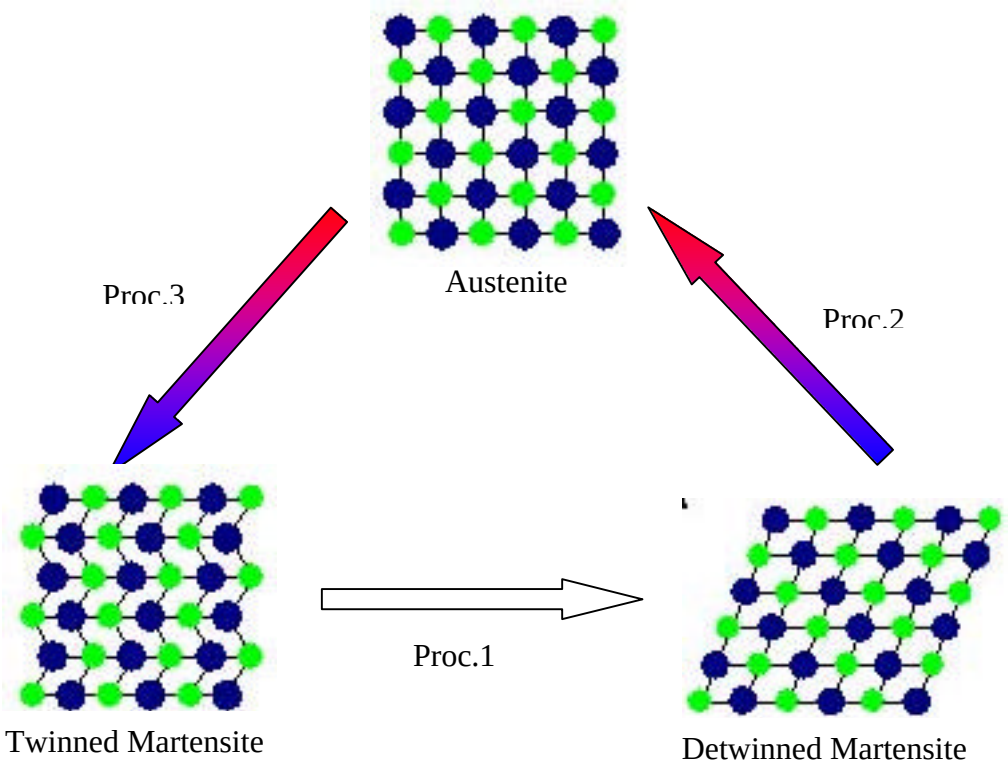

Figure 3
Transformations between different phases (Smart Lab at TAMU) ***[4]***

During Procedures 1, 2 and 3, smart material will experience external stress change, temperature increase, and temperature decrease. Finally, it will go back to its original twinned status. Constraints of Procedure 3, the recovery procedure from Austenite to twinned Martensite, will generate a considerable force. This particular property can be used in many ways in civil engineering structural applications.

Superelasticity is another important property of smart materials. When the Austenite finish temperature A_f is relatively very low, the superelasticity material will stay as Austenite under room temperature. In this Austenite phase range, the superelasticity material can transform into detwinned Martensite under stress. However, the detwinned Martensite material will go back to Austenite when the external stress is released, as indicated in figure 4.

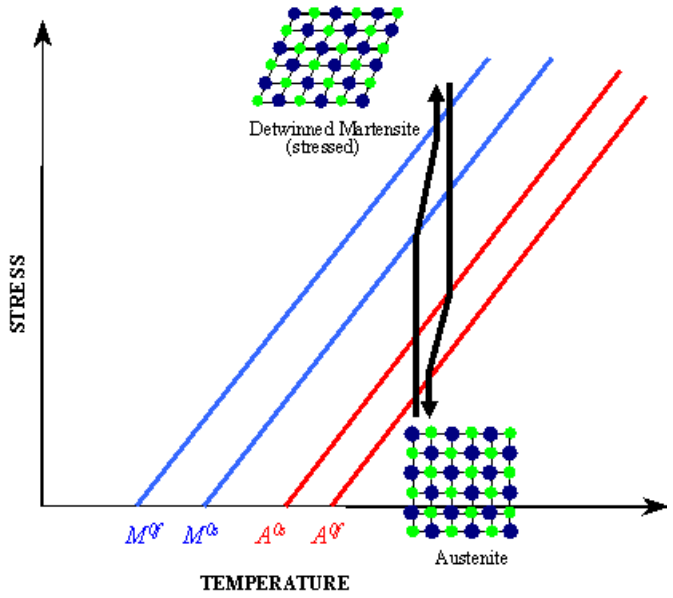

Figure 4
stress-induced transformations of Austenite materials (Smart Lab at TAMU) *[4]*

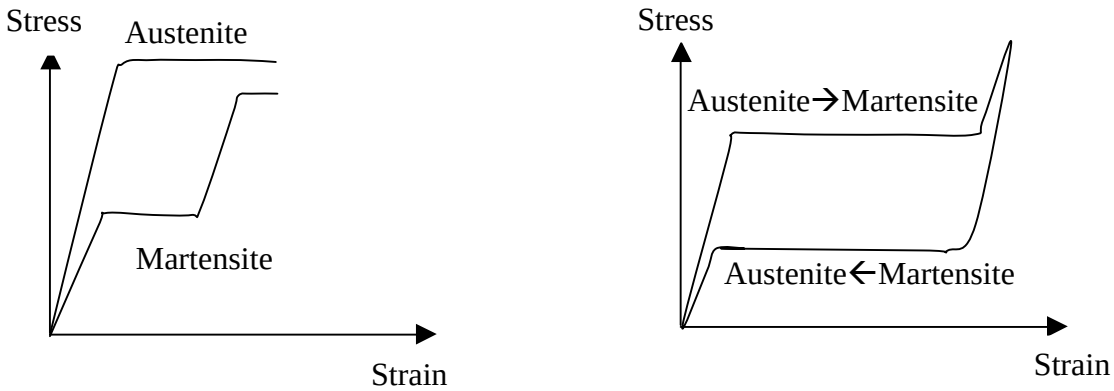

Figure 5
Stress-strain relationship of Austenite and Martensite

From the stress-strain point of view, smart materials act differently in Martensite and Austenite phases. Figure 5a shows the typical stress-strain curves of smart materials at these two phases. Figure 5b shows the stress-strain relationship of the typical phase changes of superelasticity smart materials under stress. The upper plateau represents the change from Austenite to Martensite under stress while the lower plateau represents the reverse process

with stress release. This property can be used to rehabilitate the cracking of concrete when superelasticity smart material is used as the reinforcement bar. Superelasticity material also has some other important features like hysteretic damping, highly reliable energy dissipation capacity through repeatable phase transformation, excellent fatigue properties, and good resistance to corrosion.

Smart Material Analysis Model

After they are mechanically deformed, smart materials can memorize their original configurations by heating the alloy above the transformation temperature. Through this kind of procedure, a recoverable strain as high as eight percent can be obtained. To better understand the mechanical properties of smart materials, constitutive models for smart materials are necessary.

The constitutive modeling of smart materials has been, and still is, the dominant problem for smart materials. Following is a short review for some models.

Ferroelectrics Model: Based on the thermodynamics, statistical physics and free energy in ferroelectrics and ferromagnetism, Muller et al. proposed a model *[5], [6]*. Through the extension of these relations to the constitutive modeling for smart materials, the two assumed coexisting phases for smart materials make it easy to understand the transformation and the related material behavior. However, it is possible to use the model in evaluating the properties of microstructures in various processes, while difficult to use in applications of engineering design. Following Muller's work, Falk and Hoffman improved the model *[7], [8]*. In the model proposed by Hoffman, free energy was assumed as a function of the absolute temperature and a high order of strain. Numerical results show that this model is useful in simulating the martensitic transformation; however, the computational aspects prohibit it for use in certain engineering applications.

Plasticity Model: Kafka proposed a plasticity model to describe the constitutive relations of smart materials *[9]*. This model was modified to represent the superelasticity and shape memory effect of smart materials. Brandon and Rogers introduced a model of single crystal for smart materials using experiments performed by Muller and Xu *[10]*. This model accounts for a wider range of physical phenomena than the traditional plastic phases though a dependence on the time history of strain and phase fractions. This model also works for single crystal smart materials in smooth transition process from elastic to plastic mode.

Hysteresis Model: Graesser and Cozzarelli proposed a 1-D constitutive model based on the hysteresis model of damping materials *[11]*. This model is analogous to the inelastic

formulations for creep and viscoelasticity containing a backstress. Hence, this model is able to represent elastic and inelastic states and the differences between loading and unloading in smart materials. It can also predict Austenite and Martensite twining hysteresis of smart materials.

Non-isothermal Model: Ivshin and Pence proposed this model in 1994 *[12]*. It contains the connections between the complete transformation phenomena and the arrested loading or unloading. This model also considers the transition from isothermal to adiabatic loading through the loading in a heat convective environment. Due to the fact that this model has only one variant of any phase, it will not capture certain phenomena in twining which are usually associated with the shape memory effect.

Applications of Smart Material

Smart materials have been increasingly used in many engineering fields like coupling and shape control, actuators, composites, shock absorption, damping of vibrations, automatic on-off switch and biomedical areas *[3], [13], [14], [15], [16], [17]*. Under the quasi-static conditions, smart materials have also been successfully adopted as load bearing actuators in some complex structures, such as rotor blades, submersibles, and aircraft wings *[18], [19], [20]*, etc. In the biomedical area, numerous investigators are carrying out the research of an underwater vehicle that shares agility and hydrodynamic efficiency of aquatic animals *[17]*.

Smart materials have abilities to change their material properties like Young's modulus, damping, and internal forces *[21], [22], [23], [24], [25]*. Using this feature, smart material has been integrated with composite material structures to implement control for static and dynamic performance. It was reported that the smart material characteristics could be well adjusted, which causes that certain static and dynamic characteristics of composite material structures can be set, such as maximum deflection and shape. What's more, natural frequencies and modes of vibrations, amplitudes of forced vibrations or damping properties can be tuned to the desired values *[25], [26]*. (See Appendix A for more details about some applications.)

Experimental Investigation

Basic Material Properties

After comparing different smart materials in terms of phase transformation temperature, material properties and price, Ni-Ti alloy from NDC (Nitinol Devices &

Components) and Special Metals Corporation was chosen as the material for this research (see table 1).

Table 1
Smart materials used in this research

	NDC	Special Metals
Superelasticity	SE 508	#C7-7078-2-1 # C7-7077
Shape Memory	SM495	

These smart materials have some basic mechanical properties provided by the companies, as shown in tables 2 to 4. This Ni-Ti alloy has a high elongation property, a low Young's modulus, and high ultimate tensile strength, compared with ordinary steels.

Table 2
Mechanical properties of NDC SE508 smart material

Young's Modulus (psi)	Ultimate Tensile Strength (psi)	Total Elongation	Transformation Temperature (A_f)
$6\text{-}11*10^6$	$160\text{-}200*10^3$	10%	5-18°C

Table 3
Mechanical properties of NDC SM495 smart material

Young's Modulus (psi)	Ultimate Tensile Strength (psi)	Total Elongation	Transformation Temperature (A_f)
$4\text{-}6*10^6$	$160*10^3$	10%	60°C

Table 4
Mechanical properties of Special Metals superelasticity materials

Young's Modulus (psi)	Ultimate Tensile Strength (psi)	Total Elongation	Transformation Temperature (A_f)
$12*10^6$	$100\text{-}200*10^3$	20-40%	94°C

Material Tests

In this task, the stress-strain curve was obtained and the shape memory effect was verified.

MTS Model Qtest-VII (figure 6) and its associate software TestWorks QT were used in the material tests. MTS Model Qtest-VII can do different material tests including axial tensile test, which is used in this task. The extensometer was used to measure the extension of the specific part of the sample. The software read both the loading and extension values directly. During the tests, the crosshead speed was set as 0.2 in/min, the highest load limit was set to 10,000 lb, and the highest extension limit was set to 0.4 inches. The specified length of the sample part for measuring the extension is two inches.

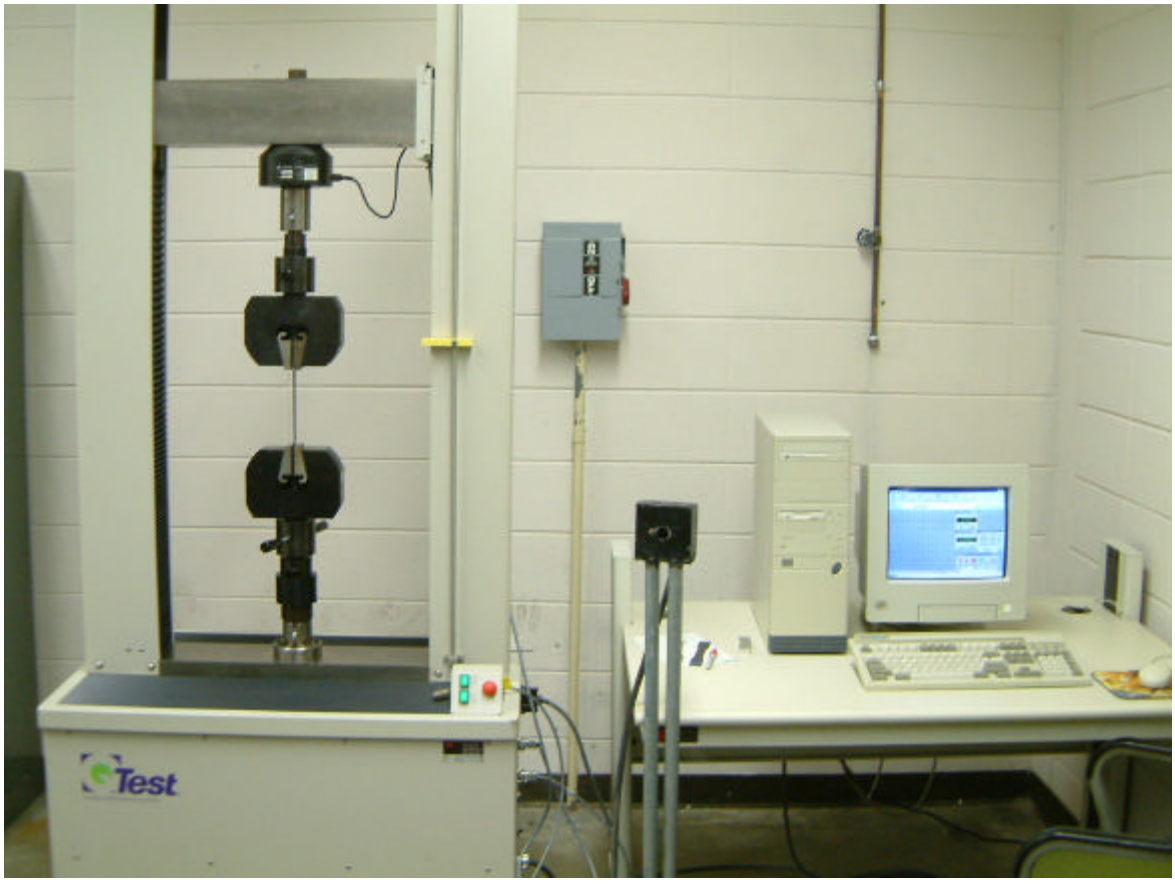

Figure 6
MTS Model Qtest-VII

Two materials were used in this task: NDC Nitinol Superelasticity SE508 wire with a diameter equal to 0.187" and shape memory SM495 wire with 0.14" diameter. All the

important material geometric parameters are listed in table 5. Since the diameters of all these materials were so small, many difficulties were encountered during the experimental investigation. For example, in the tension test, it was hard to avoid the slip between the material samples and the clamps. We sought different approaches to stop this slip, but we were unable to resolve the problem thoroughly. Another problem encountered in the beam experiment was the inability to place strain gauges on the surface of the smart material reinforcement bar. This led to the inability to measure the strain of smart material. Due to the limited resources in the availability of materials for this project, careful planning was necessary. After the shape memory material was pulled for plastic transformation, it was put into an oven. The temperature was set to 10°C above its A_f so that the shape memory material could undergo the transformation indicated in figure 3.

Table 5
Geometric properties of the materials

	Diameter (in.)	Sample Length (in.)
SE508	0.187	$6\frac{9}{16}$
SM495	0.14	$6\frac{7}{8}$

Beam Experiments

The main objective of the beam experiments in this research was to verify the auto-rehabilitation performance of concrete beams with superelasticity material as a reinforcement bar. Four concrete beams were designed according to the ACI design code. Five concrete cylinders were cast to measure the concrete compression strength as concrete beams were cast. The geometry and material information for the four beams are listed in table 6.

Table 6
Cross section and reinforcement information of concrete beams

Beam	Dimension (in) W x H x L	Reinforcement Type	Reinf. Amount (in.) (No.) D (Diameter)	Total Reinf. Area (in^2)
1	3 x 6 x 20	Regular	3D0.125	0.0368
2	3 x 6 x 20	Superelasticity	1D0.187 &2D0.120	0.0501
3	3 x 6 x 20	Superelasticity	8D0.085	0.0454
4	6 x 3 x 20	Superelasticity	2D0.187&2D0.110	0.074

From figure 7, we can see the whole arrangement of the beam experiment. Figure 8 shows the relationship between all the machines and parameters measured in the experiments. In this figure, RCLM represents recording and control of loading machine while PC means personal computer. RCLM controlled and obtained readings from the loading machine. Displacement, cracking, and strain can be measured using a data acquisition system and then transferred to the PC. Since the RCLM system and the data acquisition system were not integrated as a whole, the force reading from RCLM and other variables from data acquisition systems were not synchronous and manual work was needed in the data analysis.

Figure 7
Arrangement of the beam test

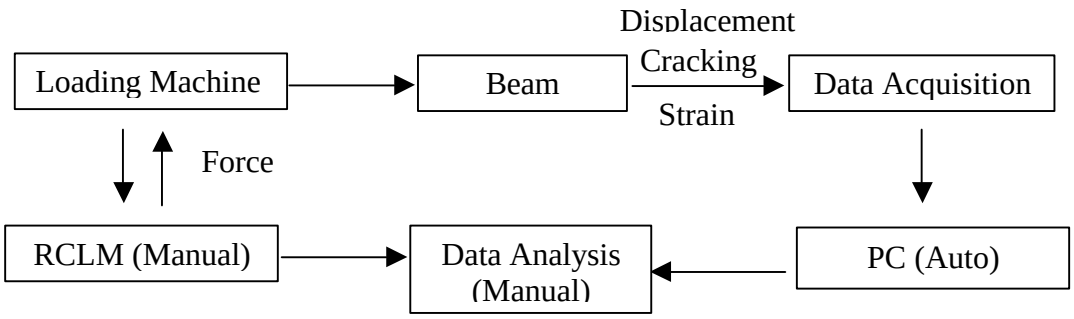

Figure 8
Flow chart of beam experiment

As shown in figure 9, GOULD data acquisition DASTARNET157 was used to read and store data during the experiments. It has up to 16 channels for strains or transducers. In this beam experiments, 4~5 strain channels were used for different beams. A displacement transducer and a cracking transducer were used for each beam experiment.

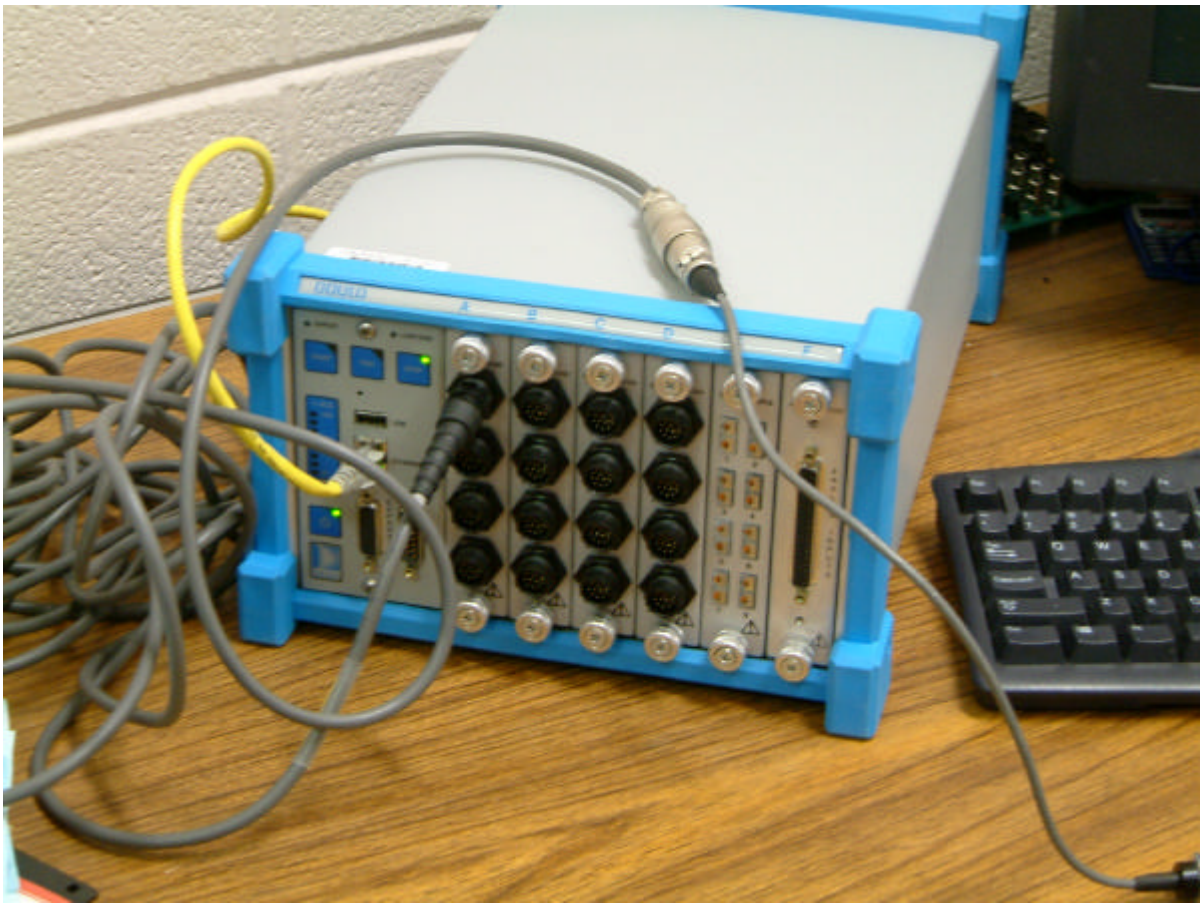

Figure 9
GOULD data acquisition DASTARNET157

As shown in figure 10, the concrete beam flexural strength test machine (RCLM in fig. 8) was used to record the force applied on the beam. This test machine was controlled manually and recorded the reading on a paper chart. It is very important to control the loading system well during the experiment.

Figure 10
Reading and loading system for the beam experiment

As shown in figure 11, the experiment beam was put on four supports (four-point loading). The middle two supports acted as the loading points, while the two ends separated from the bottom of the beam when the force was applied upward. On top of the beam, the two blocks can move up and down, working as two constrains. In addition, the displacement transducer and cracking transducer on the top of the beam can be seen in figure 11.

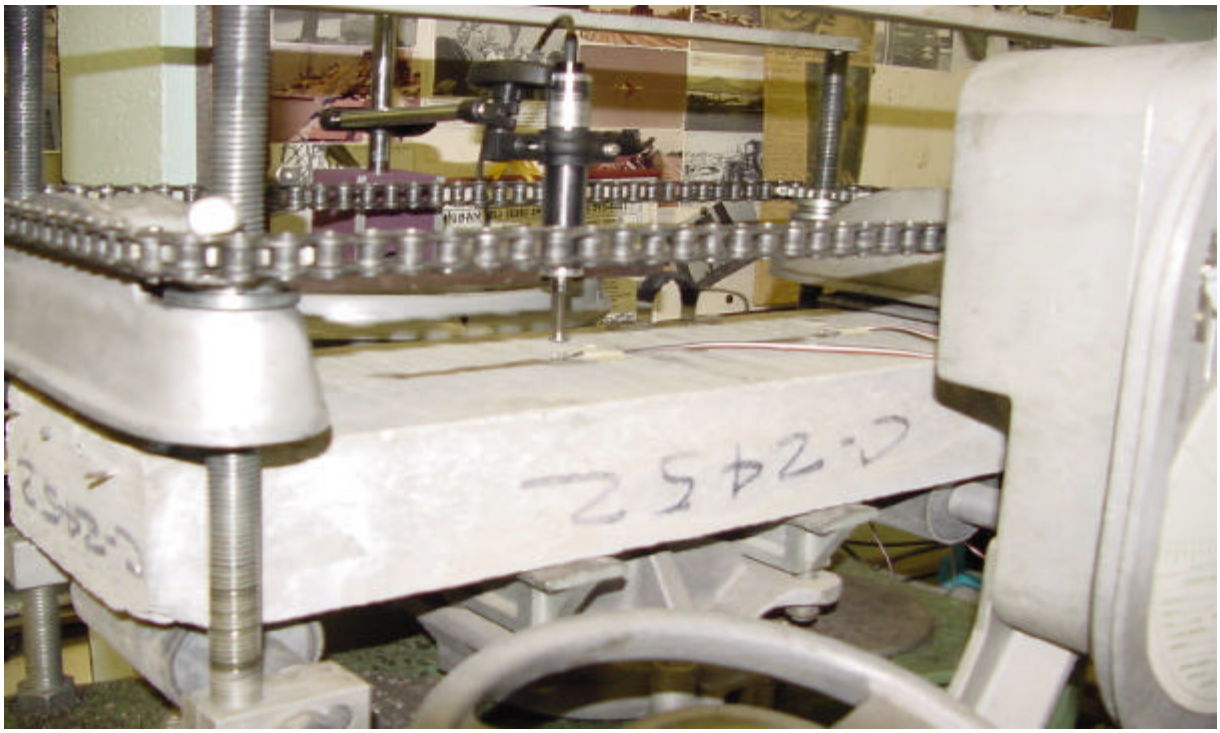

Figure 11
The arrangement of the beam

The calculation model for the beam is shown in figure 12.

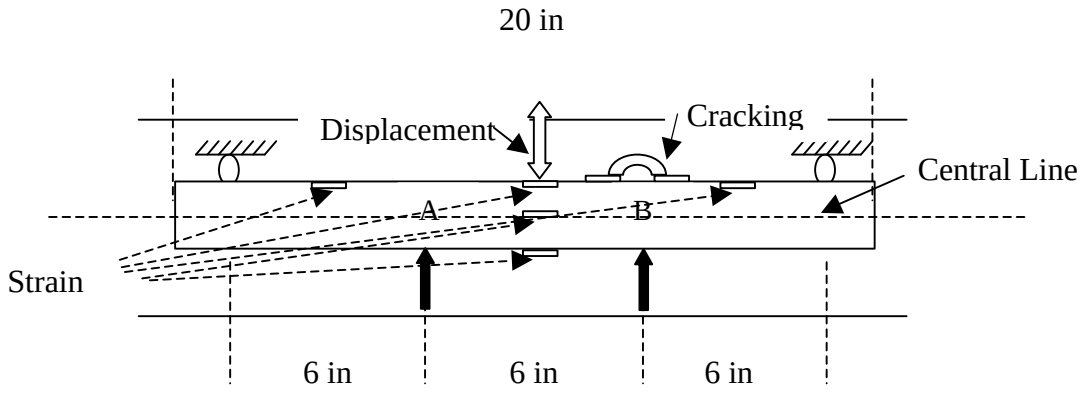

Figure 12
Calculation model for the beam

From the geometric and material parameters listed in the previous tables, the theoretical cracking moment, ultimate moment, and strains at different points on the surface of the concrete beams can be calculated after the compression strength is obtained from concrete tests. According to this information, loading and unloading procedure can be developed before beam experiments. For each beam, 3~4 loading-unloading circles were carried out to observe the cracking moment, the change of cracking width, and the other performance measures of the beams. In the first loading circle, the external force was incrementally applied until the first cracking of concrete occurred. The force was then reduced to zero. In the second and third loading circles, the external force was added to enlarge the existent cracking, and then it was reduced to zero. In the fourth loading, the external force was increased all the way to crush the beam. In the test process, the width of the cracking was manually recorded at certain loadings; while the displacement of the mid-span, the cracking transducer, and the strains at several points were recorded throughout the entire test.

DISCUSSION OF RESULTS

Results of Material Tests

Figure 13 shows the load-extension curve and figure 14 shows the stress-strain curve for NDC superelasticity material SE508 wire with a diameter of 0.187''. In figure 14, the yield stress of NDC superelasticity material is about 80,000 psi, which is higher than the value of 65,000 psi given by the company. From the data, the Young's modulus can be calculated as $18.54*10^6$ psi, which is higher than $6\text{-}11*10^6$ psi provided by the company.

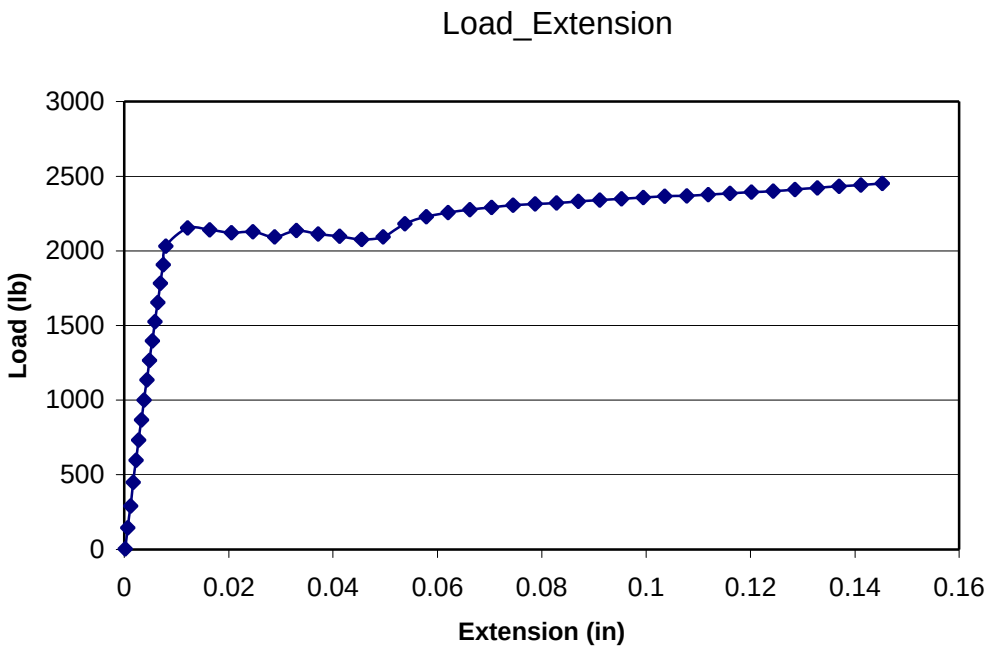

Figure 13
Load-extension curve for NDC superelasticity material width = 0.187"

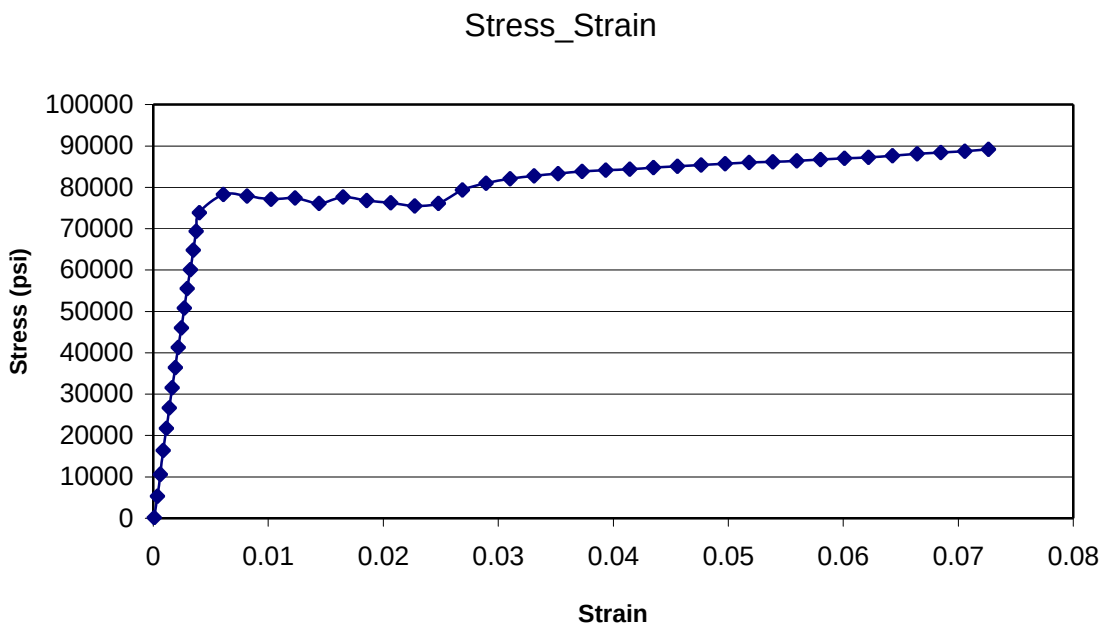

Figure 14
Stress-strain curve for NDC superelasticity material width=0.187"

Figures 15 and 16 show the corresponding curves for NDC shape memory SM495 wire with a diameter of 0.14". In figure 16, the plateau reading of stress-strain curve is about 13,500 psi, which is close to the 15,000 psi provided by the company. The Young's modulus calculated from this figure is $8.14*10^6$ psi, while the one provided by the company is $4\text{-}6*10^6$ psi.

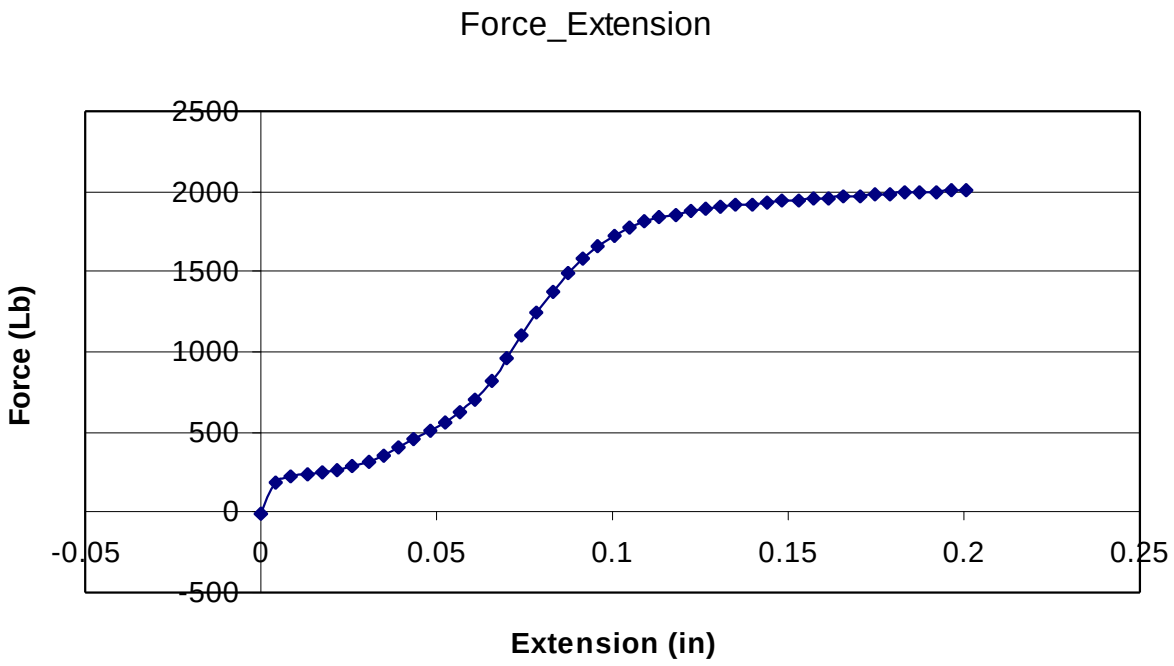

Figure 15
Load-extension curve for NDC shape memory width =0.140"

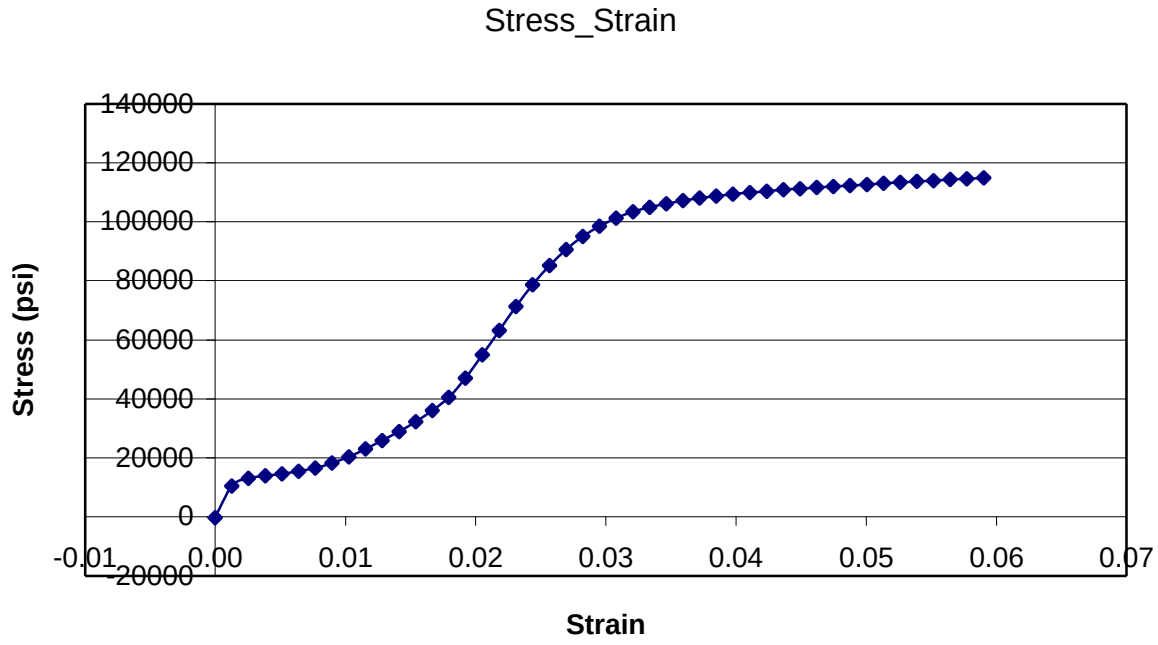

Figure 16
Stress-strain curve for NDC shape memory with d=0.140"

The strength calculated from test data is close to the value provided by the company, while the Young's modulus is larger than the value. The reason may be that since the sample is very small and the surface is very smooth, the slipperiness exists not only between the extensometer and the sample, but also between the clamp and the sample. The reading of force will not be affected though there is slipperiness between the clamp and the sample, while the reading of the extension will be less than the actual value. Considering the two factors, the calculated Young's modulus should be greater than the actual one.

The stress-strain curve of the superelasticity material (figure 14) and the one for the shape memory material (figure 16) fit figure 5a well. In the previous figures, the shape memory material has a post-yield period with much higher strength than the yield strength.

After the NDC shape memory material is pulled, it is put into the oven as illustrated in the methodology. Because the shape memory material has been over-stretched into this strengthened period (due to the slipperiness, it was very difficult to control the pulling), it could not go back to its original length by heating it.

Results of Beam Experiments

Before the beam experiments, compression tests of concrete cylinders were carried out. In these compression tests, the average concrete strength at 28 days was 3810.5 psi.

From the material and geometric parameters listed in the methodology part, the theoretical cracking moment and nominal moment were calculated, following the ACI code. In Table 7, M_c = cracking moment, M_n = nominal moment, and P_c and P_n are the forces corresponding to M_c and M_n, respectively. Those pre-calculated moments and the associated forces are helpful to control the loading process.

Table 7
Cracking moment and nominal moment of beams

	Beam 1	Beam 2	Beam 3	Beam 4
M_c (lb?in)	8662.1	8570.7	8548.8	4342.7
M_n (lb?in)	11880.8	20006.6	18108.9	10134.9
P_c (lb)	1443.7	1428.45	1424.8	723.7
P_n (lb)	2464.3	3334.4	3018.2	1689.1

The four beam experiments were done in sequence. These experiments went well except for the control beam. Because of the improper operation of the data acquisition

during the experiment for the control beam, it failed to record the experimental data. For all the four beams, only one major visible crack appeared for each beam during the whole loading process. This was partially due to the slipperiness between the wire and the concrete, which prevented the development of uniformly distributed cracking typical of reinforced concrete beams. High pitch noise could be heard, and the slipperiness of the wires was obvious since the wire ends were observed moving into the concrete. This serious problem may have contribution to some of the anomalous results discussed later.

From the theory of simple beams, the cracking should have appeared at the top surface of either one of the two supports (figure 12) since the load was applied upward and the bending moment at mid-span was less than that at the loading section due to the downward self-weight effect. In the actual experiment, the cracking did appear at one of the two supports on all the beams except the fourth, which appeared in the constant moment range (figure 17). We had only one cracking transducer available. Since the first cracking could appear at either point A or B randomly in every beam test (figure 12), we had to measure the width of cracking through the cracking transducer by chance. Unfortunately, we missed the first cracking each time.

Figure 17
The cracking appears at the middle span of the fourth beam

Following are the recorded experimental data from the other beams. The data acquisition recorded data such as strain, displacement, and cracking versus time. Force was manually recorded through the paper chart reading since no load cell was available at that time. Therefore, the relationship between the force and strain, displacement, or cracking cannot be directly established.

Results and Discussions of the Second Beam

As indicated in figure 18, five strain gauges were installed on the surface of the concrete beam. Three of them were on the top, numbered one to three; point four was on the central line and point five was near the bottom of the beam.

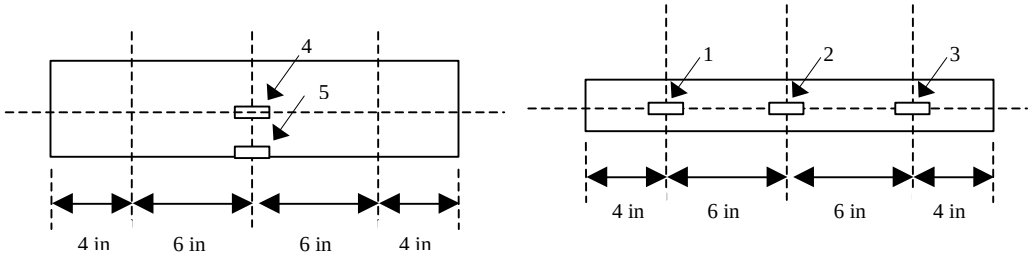

Elevation

Plan View

Figure 18
Layout of strain gauges of the second beam

Because the RCLM and the data acquisition worked separately, the connection between force and the other parameters cannot be built directly. The results of the second beam are plotted in figure 19, using time as its X-axis.

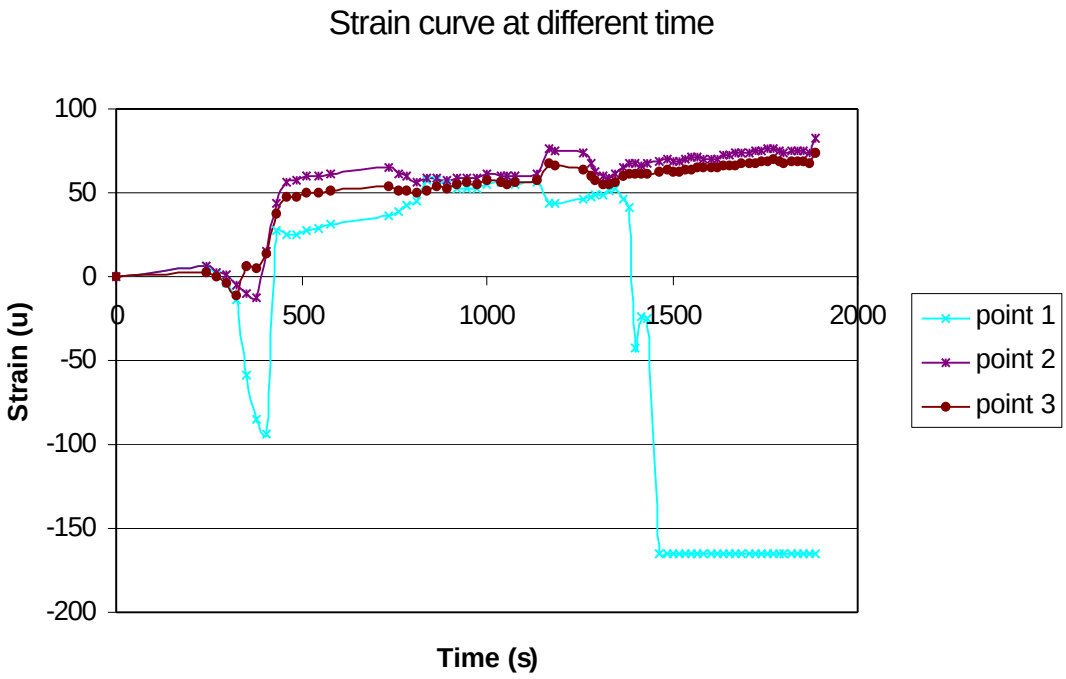

Figure 19
Strain versus times for the second beam

To explain the curve of point 1, it is obvious that the cracking through this strain gauge at the late stage changes the reading largely. The data acquisition device stops to read the strain after the strain reading is out of range, which in this case is -150 u.

Results and Discussions of the Third Beam

For the third beam, four instead of five strain gauges were installed on the surface of the concrete beam, as figure 20 indicates. The force-displacement is plotted in figure 21. In this figure, the trend for the curve is good, but for the data from 0 to 500 pounds, there is some discontinuity in every circle. In the first circle, force was added up to 1850 pounds and then the first cracking appeared. Then the force was reduced to zero, as indicated in figure 21. The plot of the first circle is difficult to explain. The peak force appeared in the second circle with a value of 3,400 pounds, which is a little higher than the calculated value in table 7. The plot of the third circle indicates that there was a sudden reduction of the displacement when the force was reduced to zero.

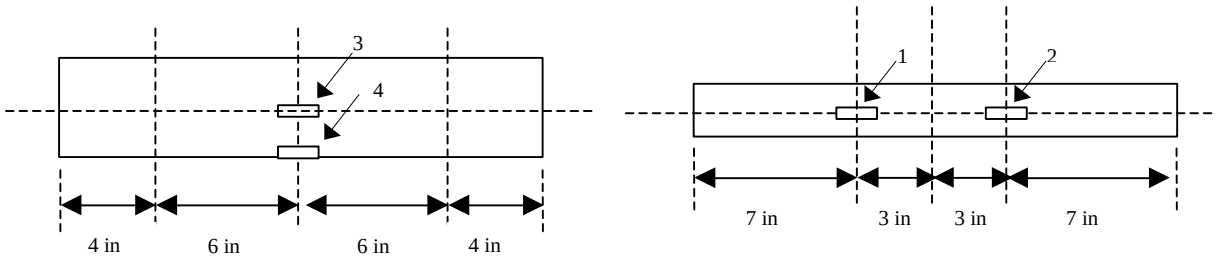

Elevation Plan View

Figure 20
Layout of strain gauges of the third beam

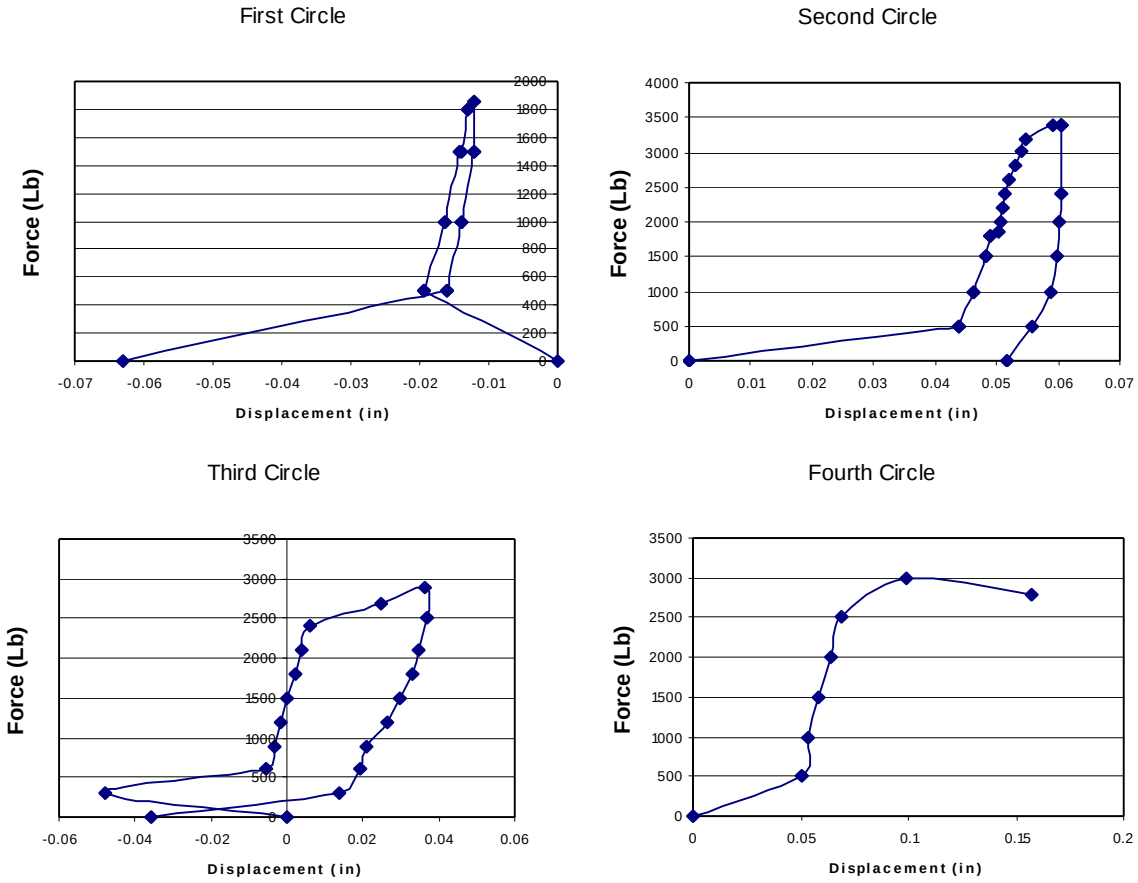

Figure 21
Displacement at the mid-span of the third beam

The strains at different points as figure 20 indicates are shown from figure 22 to figure 25. In the plot of the first circle in figure 22, the strain goes back further than the

original place, possibly because it was hard to control the unloading speed in the beam experiment. In the second circle, when the peak force was reached, the force was held for a while. At that time, the strain was reduced automatically. Since the strain rehabilitation finished during the constant peak force, the strain was kept almost constant when the force was reduced. When the force was reduced to zero, there was some residual strain because the concrete had cracked already.

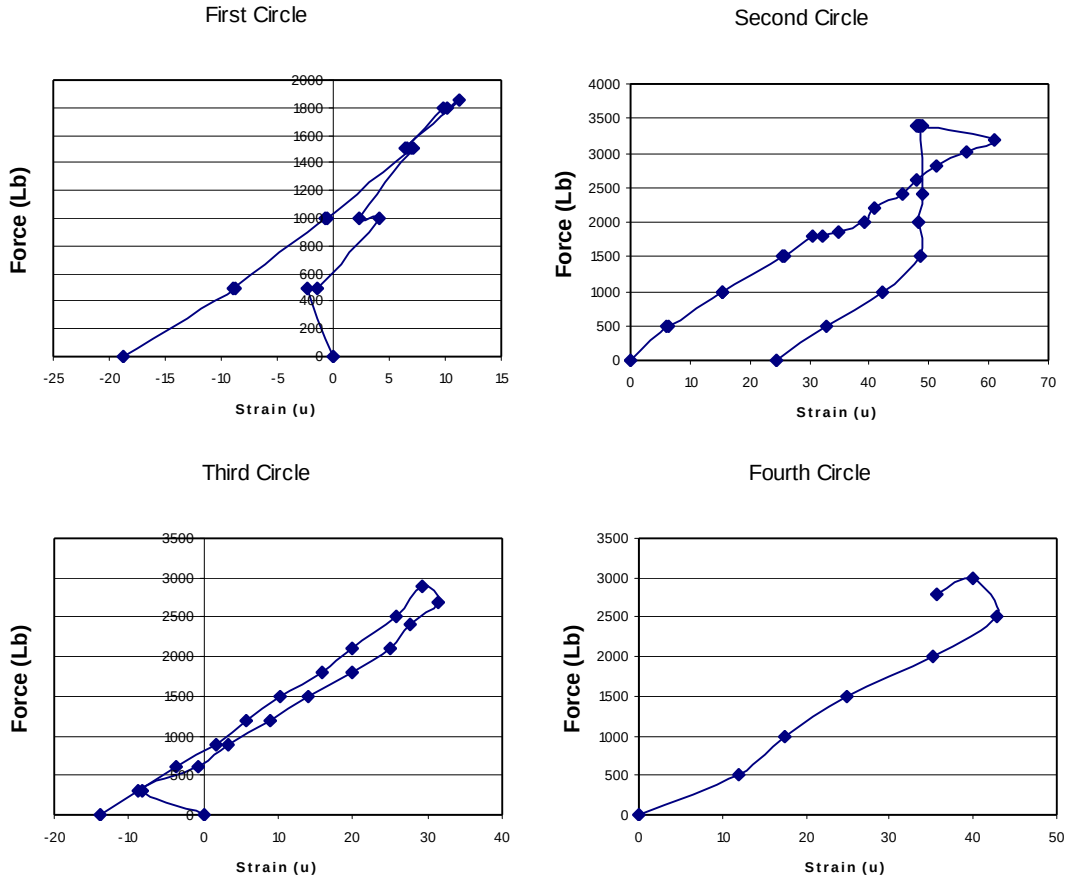

Figure 22
Strain at point 1 for the third beam

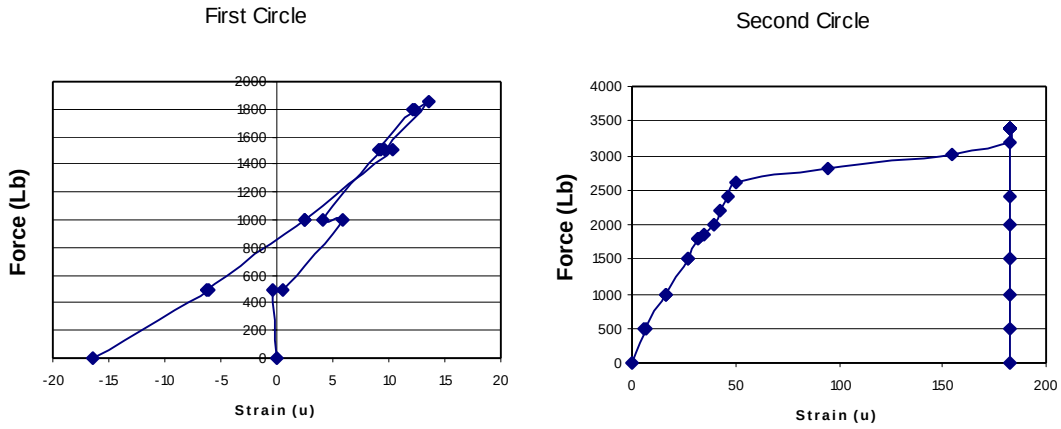

Figure 23
Strain at point 2 for the third beam

In figure 23, the main cracking is through the strain gauge, which caused the strain reading to be out of range. Thus, the data acquisition device could not record it correctly after 3,000 lbs. We would like to point out that in the first circle, the strain readings of point 1 and point 2 are similar.

There are some non-zero readings of the strain gaugeat pont 3 (figure 24) on the central line of the cross section (neutral axis position) for the third beam;however, the average and the standard deviation of the strain gauages are not large.

There are some non-zero readings of the strain gauge at point 3 (figure 24) on the central line of the cross section (neutral axis position) for the third beam; however, the average and the deviation of the strain readings are not large.

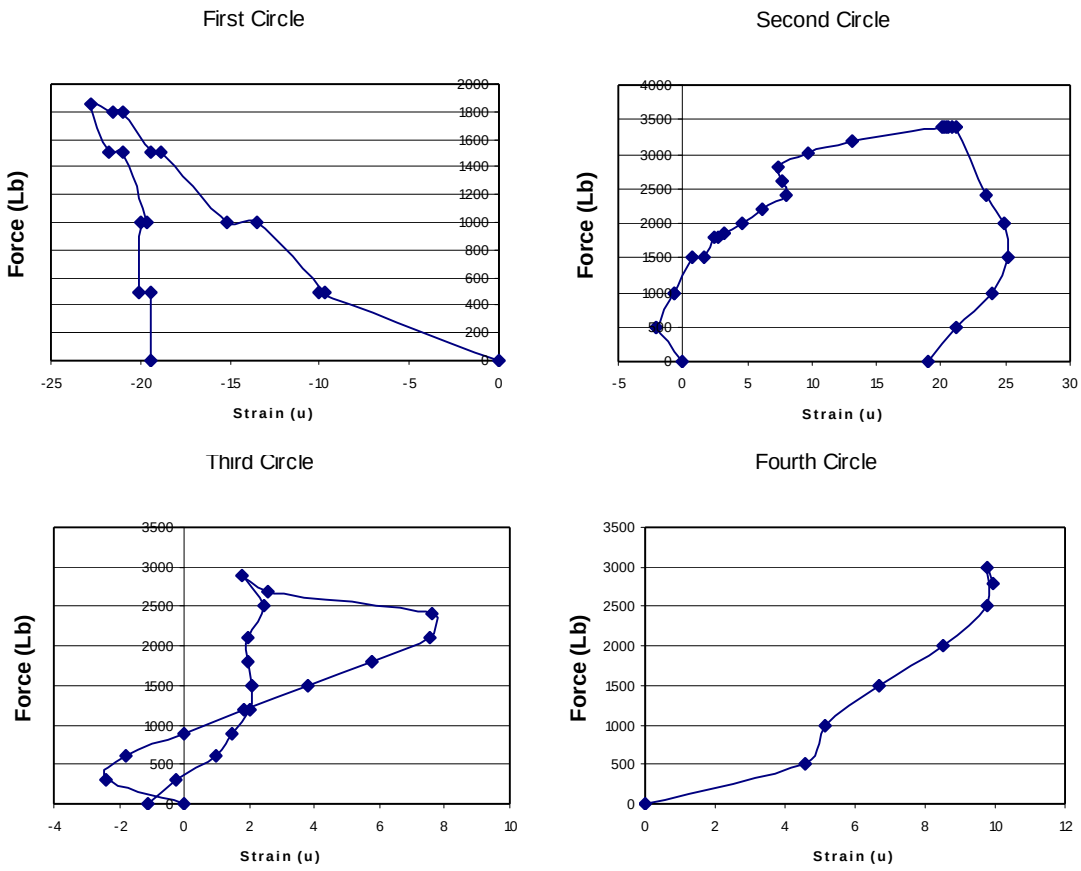

Figure 24
Strain at point 3 for the third beam

The reading of the strain gauge at point 4 (figure 25) at the bottom of the third beam is almost the negative of the reading at point 1.

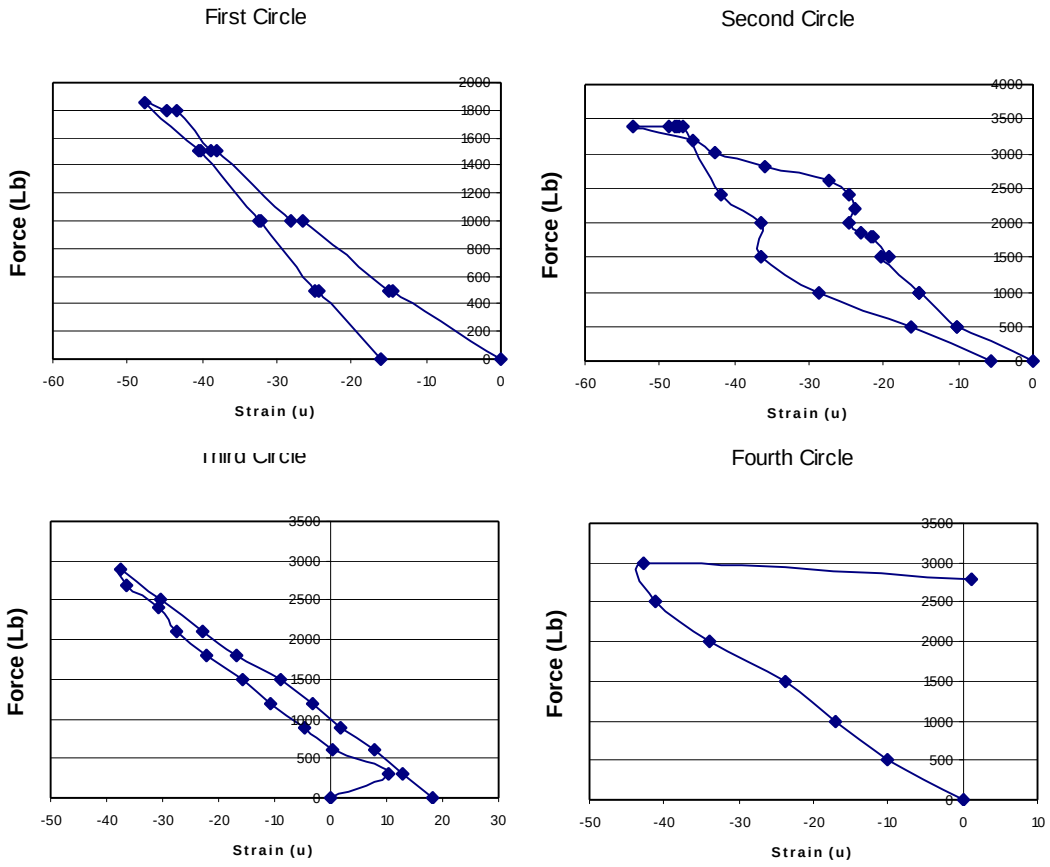

Figure 25
Strain at point 4 for the third beam

During the whole circle of loading and unloading, the cracking width was read at some loading steps since the cracking did not pass the transducer. Table 8 includes the cracking width read manually at some loading steps.

Table 8
Cracking width at some loading steps

3,400 lb, second circle	2,900 lb, third circle	0 lb, third circle
0.01 in	0.05 in	0.03 in

Although 3,400 pounds is the peak loading force, its cracking width is not the largest. Damage increased in the repeated loading circles. The cracking width reached 0.05 inches at 2,900 pounds in the third circle, which was much bigger than the one at 3,400 pounds peak force after the second circle. When the force was reduced in the third circle, the cracking

width was also reduced. The reduction of the cracking width should be partly due to the force of gravity of the concrete itself, but mainly due to the self-rehabilitation of the superelasticity material.

Results and Discussions of the Fourth Beam

The layout of strain gauges in the fourth beam is the same as the third beam, except that the fourth beam is a flat beam, as figure 26 indicates:

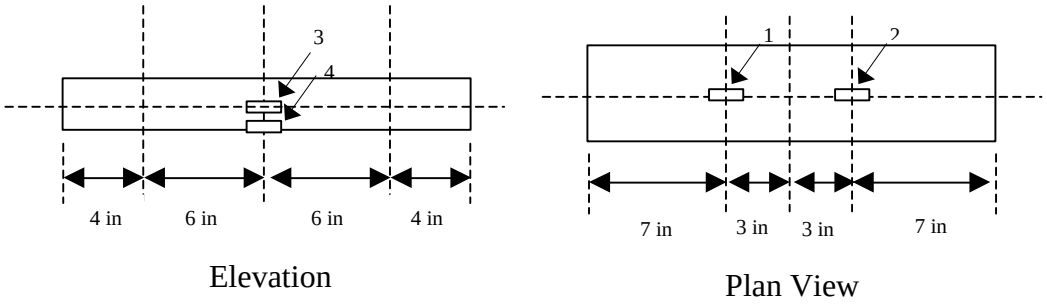

Figure 26
Layout of strain gauges on the fourth beam

There are three loading and unloading circles in the fourth beam experiment. Figure 27 shows that the beam with the smart material has good ductility since it can sustain displacement up to 10 mm. In addition, there is some discontinuity between zero loading and 400 pounds loading. Compared to the third beam, the area between the loading and the unloading curve of this beam is bigger. It is easy to understand this phenomenon, however, since this beam has more superelasticity material and thus a larger capacity of dissipating energy.

As with the previous two beams, the crack width reading of the fourth beam should be considered useless because no cracking is through the cracking transducer (Appendix).

Figures 28 through 31 are strain readings at different places, as indicated in figure 26.

While these figures provide almost the same conclusions as those of the third beam, there are two differences. First, the cracking appeared through the constant moment range, which was between the two middle supports, instead of above the middle supports. This was possible since the self-weight is very small, compared with the external force. Second, the peak reading of strain at point 4 was almost twice that of point 1 or point 2.

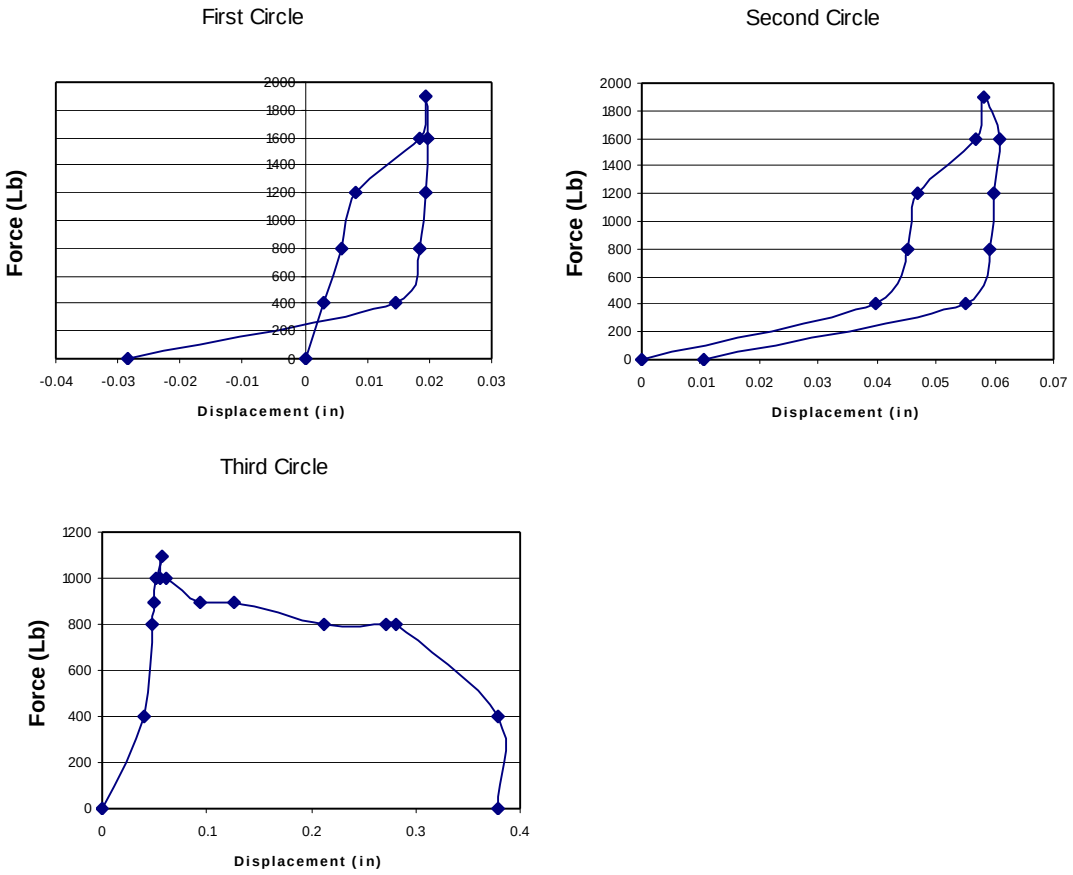

Figure 27
Displacement at the middle span for the fourth beam

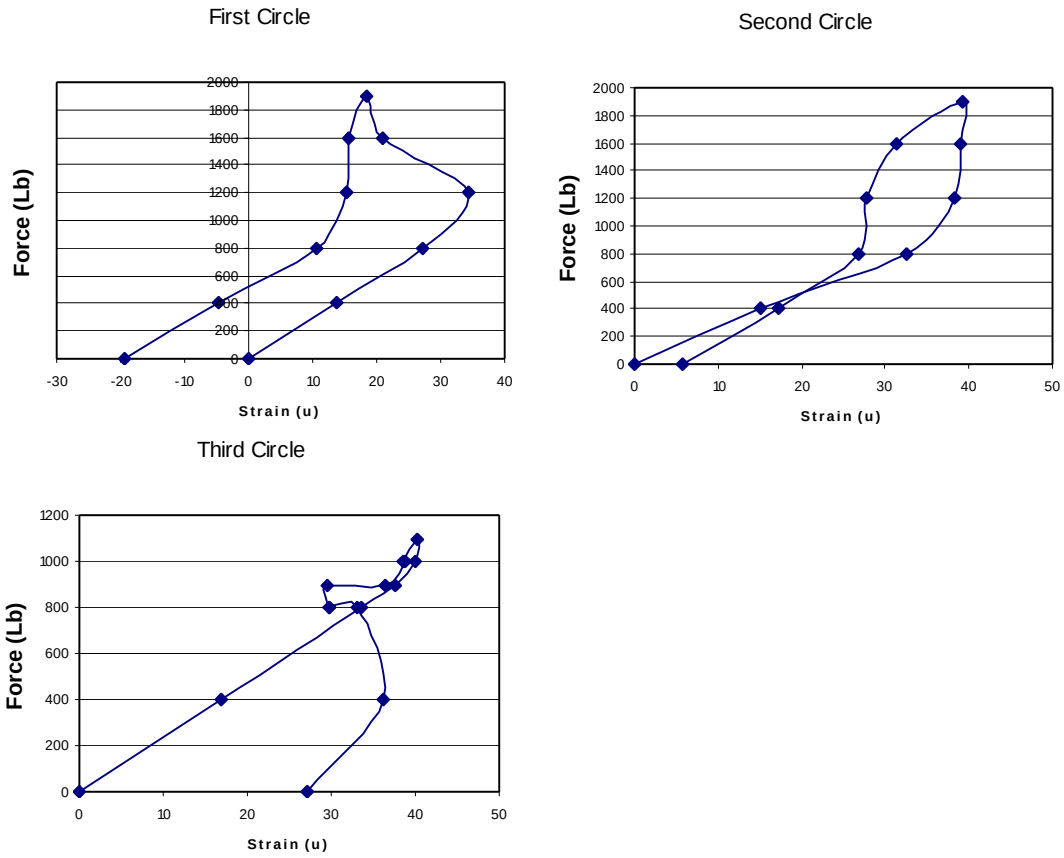

Figure 28 Strain at point 1 for the fourth beam

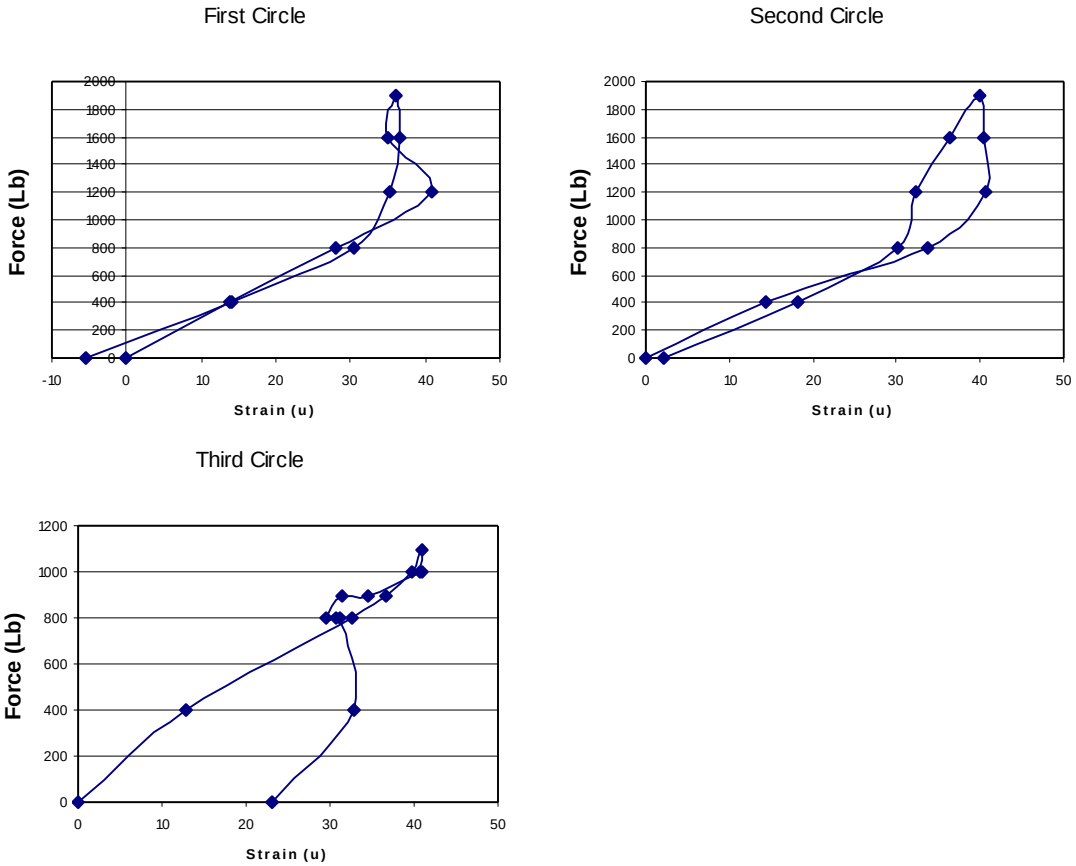

Figure 29
Strain point at point 2 for the fourth beam

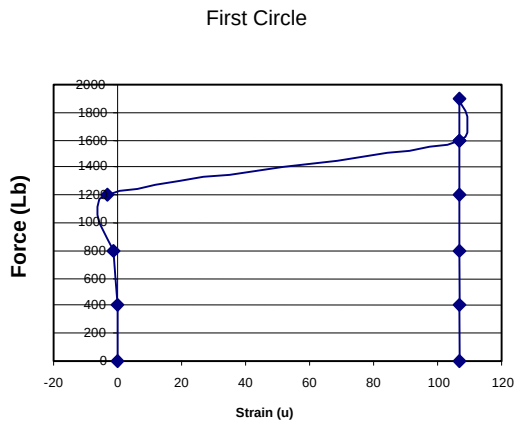

Figure 30
Strain at point 3 for the fourth beam

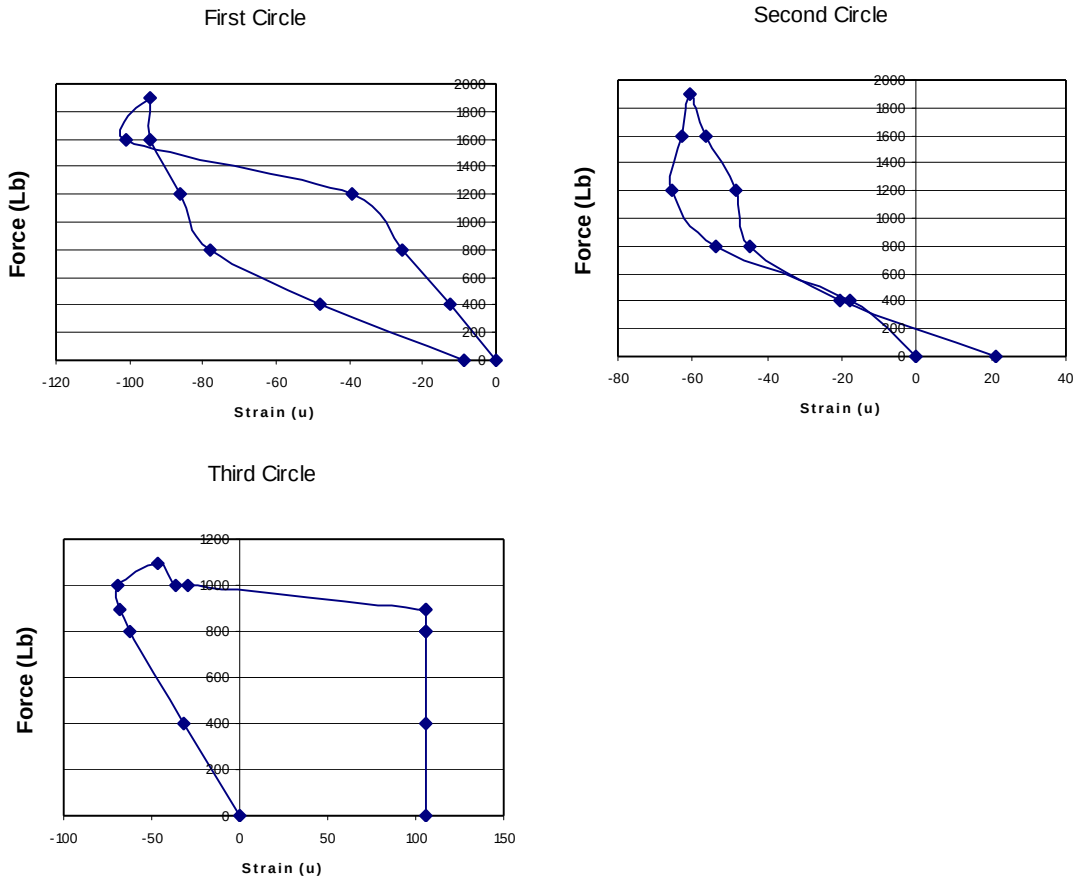

Figure 31
Strain at point 4 for the fourth beam

CONCLUSIONS

From results and discussions in the previous sections, conclusions can be drawn as follows:

The literature review indicated that smart materials have shown their promise in civil engineering applications and some research has been conducted in this area.

The basic mechanical properties of smart materials, including superelasticity and shape memory, were obtained from the material tests, especially the force-extension and stress-strain curves. Those curves matched well the general properties described in the literature (figure 5).

The superelasticity material tested had high yield strength so that under ordinary force the material will still be elastic. Therefore, it can go back to the original shape after the force (or stress) is released. Beyond that stress, the recovery will depend on the phase change.

From the results of the beam tests, the superelasticity material recovered the concrete cracking to some extent after the external force decreased. However, the gravity may have also affected the results. More careful experimental design is needed.

The wire surface's slipperiness was very serious in both the pulling test and the beam test; this problem contributed to the cause of many anomalous results.

RECOMMENDATIONS

From the previous experimental investigations and results, the following recommendations can be made:

- Superelasticity smart material has the ability to go back to its original length due to stress-induced phase changes. Therefore, it may be used as self-rehabilitation material in concrete beams. However, it is not efficient to build the wires/strands into the concrete. Instead, superelasticity smart material should be used as external reinforcement.

- Currently, smart materials are not developed specifically for civil engineering applications, and it is very difficult to acquire appropriate materials for these applications, considering the required surface conditions, diameters, and phase transformation temperatures. In addition, material cost is still too high; therefore, it is not recommended for actually large-scale (mass) applications at this time.

- Research is needed to identify some local applications that need small amounts of smart materials. One potential application is for dynamic damping.

- This research is just the first step in the investigation of the application of smart materials in structural engineering. Some larger beams using smart materials as external prestressing/reinforcing will be prepared for further experimental study.

- There are many other research and application areas worth of investigating, such as shape memory effect on beams, two-way training, two-way effects on beams, etc. However, these studies may require more financial resources and present more technical challenges.

REFERENCES

1. Hodgson, D.E., and Brown, J.W. “Using Nitinol Alloys,” Report of Shape Memory Applications Inc., 2000.

2. Maji, A.K., and Negret, I., “Smart Prestressing with Shape-memory Alloy.” *Journal of Engineering Mechanics*, Vol.124, No.10, Oct. 1998, pp.1121-1128.

3. DesRoches, R., “Application of Shape Memory Alloys in Seismic Rehabilitation of Bridges,” Technical Report NCHRP-IDEA project 65, Feb. 2002.

4. Lagoudas, D.C., “Introduction to Shape Memory Alloys,” Smart Lab at TAMU, http://martensite.tamu.edu/overview/overview.html. Dec. 2002.

5. Muller, I., “A Model for a Body with Shape Memory.” Architecture Rational Mechanics Analysis, Vol. 70, 1979, pp.61-77.

6. Muller, I., and Wilamski, K., “A Model for Phase Transformation in Pseudoelastic Bodies.” *I1 Nuova Cimento*, 57B, 1980, pp.238-318

7. Falk, F. “Model Free Energy, Mechanics, and Thermodynamics of Shape Memory Alloys.” *Acta Metallurgica et Materialia*, Vol. 28, 1980, pp.1773-1780.

8. Hoffman, K.H., and Zheng, S.M., “Uniqueness for Nonlinear Coupled Equations Arising from Alloy Mechanism,” Technic Report No.14, Center for Applied Mathematics, Purdue University, 1986.

9. Kafka, V. *Inelastic mesomechanics*. World Scientific Publication, Co., Singapore, New Jersey, Hong Kong, 1987.

10. Brandon, D., and Rogers, R.C., “Constitutive Laws for Pseudo-elastic Materials.” *Journal of Intelligent Material Systems and Structures*, Vol.3, 1992, pp.333-346.

11. Graesser, E.J., and Cozzarelli, F.A., “Extension of a One-dimensional Model for Hysteresis to Three Dimensions: Procedure and Verification, High Temperature Constitutive Modeling: Theory and Experiment,” Ph.D dissertation, State University of New York at Buffalo, New York, 1990.

12. Ivshin, Y., and Pence, T.J., “A Thermomechanical Model for a One Variant Shape Memory Materials.” *Journal of Intelligent Material Systems and Structures*, Vol. 5, 1995, pp.455-473.

13. Harrison, J.D., and Hodgson,D. E., “Shape Memory Effects in Alloys,” Plenum Press, 1975, pp.517.

14. Liang, C., and Rogers, C.A.. “One-dimensional Thermomechanical Constitutive Relations for Shape Memory Materials.” *Journal of Intelligent Material System and Structures*, Vol.1, 1992, pp.207-234.

15. Ghandi, K., “Shape Memory Ceramic Actuation of Adaptive Structures,” Master thesis, MIT, 1995.

16. Soroushian, P., and Hsu, J.W., “Superelasticity-Based Rehabilitation and Post-Tensioning of Bridge Structures,” NCHRP-96-IDO29, NCHRP-IDEA, Aug. 1997.

17. Lagoudas, D., Rediniotis, O.K., and Khan, M.M.. “Applications of Shape Memory Alloys to Bioengineering and Biomedical Technology.” *Proceeding of 4th International Workshop on Mathematical Methods in Scattering Theory and Biomedical Application*, Perdika, Greece, Oct. 1999, pp.195-207.

18. Liang, C., Davidson, F., Schetky, L.M., and Straub, F.K.. “Applications of Torsional Shape Memory Alloy Actuators for Active Rotor Blade Control-opportunities and Limitations.” *SPIE Proceedings of Mathematics and Controls in Smart Structures*, Vol. 2717, 1996, pp.91-100.

19. Garner, L.J., Wilson, L.N., Lagoudas, D.C., and Rediniotis, O.K.. “Development of a Shape Memory Alloy Actuated Biomimetic Vehicle.” *Journal of Smart Materials and Structures*, 9, 1999, pp.673-683.

20. Jardine, A.P., and Kudva, J.M., Martin, C., and Appa, K.. “Shape Memory Alloy Ti-Ni Actuators for Twist Control of Smart Wing Designs.” *SPIE Proceedings of Mathematics and Controls in Smart Structures*, Vol. 2717, Feb. 1996, pp.160-165.

21. Otsuka, K., and Wayman, C.M., *Shape Memory Materials*, Cambridge University Press, Cambridge, 1998.

22. Ford, D.S., and White, S.R.. “Thermomechanical Behavior of 55Ni45Ti Nitinol.” *Acta Metallurgica et Materialia*, Vol. 44, No. 6, 1996, pp.2295-2307.

23. Piedboeuf, M.C., Gauvin, R., and Thomas, M.. “Damping Behavior of Shape Memory Alloys: Strain Amplitude, Frequency and Temperature Effects.” *Journal of Sound and Vibration*, Vol. 214, No. 5, 1998, pp.885-901.

24. Gandhi, F., and Wolons, D., “Characterization of the Pseudoelastic Damping Behavior of Shape Memory Alloy Wires Using Complex Modulus.” *Journal of Smart Material Structures*, Vol. 8, 1999, pp.49-56.

25. Rogers, C.A., Baker, D.K. and Jaeger, C.A., “Introduction to Smart Materials and Structures, Smart Materials, Structures, and Mathematical Issues.” Technomic Publishing Company, Inc. 1989.

26. Fuller, C.R., Elliott, S.J., and Nelson, P.A., *Active Control of Vibration*. Academic Press Ltd., London, 1996.

27. Soroushian, P., Ostowari, K., Nossoni, A. and Chowdhury, H., “Repair and Strengthening of Concrete Structures through Application of Corrective Post Tensioning Forces with Shape Memory Analysis.” In the Transportation Research Record 1770, TRB, National Research Council, Washington, D.C., 2001, pp.20-26.

APPENDIX

A. Applications of Smart Materials

As described in the literature review, smart materials have increasingly been used in many engineering fields. In this part, some innovative applications in civil engineering are summarized as follows.

Seismic Rehabilitation of Bridges *[3]*

Seismic damping devices were built with shape memory alloys that can be applied to retrofit bridges. By concentrating energy dissipation in controlled locations, these devices can be used to reduce the demand on individual frames in a multi-frame bridge, thereby enhancing the performance of these structures.

Optimization of Smart Material Properties: The work was carried out in several steps. The first step is to evaluate the effects of thermo-mechanical processing on the characteristics of Nitinol bars and the evaluation of effects of the bar diameter, loading frequency and temperature on the characteristics of Nitinol bars undergoing tension and compression cycles. Studies show that the effect of load frequency, within the range expected for seismic applications, is small. The ambient temperature has little effect on damping characteristics. Comparing the energy dissipated and the residual strain in the samples, it is found that annealing a temperature of 350°C is the optimal temperature for all four cases. The energy dissipated per unit mass of material was greatest for the samples at 350°C. The sample treated at 450°C had by far the worst performance in terms of energy dissipation. Another parameter, which is important in the structure as well as reduced energy dissipation capacity for applications in seismic mitigation, is the residual strain in the smart material bar. Ideally, the sample should have very small residual strains after repeated cycles. Large residual strains lead to large displacements. Results also showed that the samples treated at 350°C have the smallest residual strain.

It was believed that the lack of information on large section behavior of smart materials is a fundamental reason that smart materials have not been implemented in structures as seismic dampers. It is generally thought that large section rods do not exhibit the same energy dissipating characteristics as smaller sections, although few studies exist to quantify this assumption. Full-scale smart material restrainer is tested, which consists of a 305 mm long, 25.4 mm diameter Nitinol shape memory alloy bar. The smart material bars are fully annealed and 25% cold-worked. The samples are threaded at the ends and vacuum annealed at 450°C for 60 minutes, followed by water quenching. The test suggested that the

nearly perfect superelastic behavior could be obtained when the bars are properly heat-treated. This leads to the potential application of using smart materials as dampers in large-scale structures, like bridges.

Application of Smart Material Restrainers to Multi-Span Bridges: Unseating of simple spans and frames has been a major problem for bridges in recent earthquakes such as the 1989 Loma Prieta, 1994 Northridge, 1995 Kobe and 1999 Taiwan earthquakes. The relative displacement of multiple-span simple supported bridges at the hinges and abutments can result in collapse of the bridge if it exceeds the allowable displacement. The use of smart material restrainers can provide a more effective alternative for limiting relative hinge displacement than traditional cable restrainers. It also provides sufficient stiffness and damping to limit the relative hinge displacements below a pre-determined value. Analytical studies of typical bridges with the smart material restrainers were conducted to evaluate the effectives of the smart material restrainers in limiting the relative displacement of the hinges in bridge decks. With experimental results from step one, nonlinear analytical models of the bridges are developed. Strong ground motions are used to simulate the effects of the smart material restrainers on the response of the bridge.

The comparison between the smart material restrainer and commonly used steel restrainer cables was made. For the bridge subjected to El Centro ground motion record, the adoption of traditional restrainer may reduce the relative displacement to 24%, while smart material based restrainer can reduce it up to 42%. There are several reasons to achieve such performance: the restrainer is superelastic and they have the ability to maintain their effective stiffness for repeated cycles. Another reason for that smart material restrainers are effective in limiting the relative displacement of the bridge deck is believed to be the energy dissipation by the restrainers. The comparison shows the energy dissipated by the smart material restrainers are 15% more than the traditional cables.

Repair and Strengthening of Concrete Structures *[26]*

Structural deficiencies of bridges caused by damaging load and environmental effects, faulty design practices or increased traffic loads represent a major problem with the US transportation infrastructure. The shape memory-based rehabilitation system promises to provide a rapid, efficient and low-cost approach with high levels of safety and reliability for the rehabilitation of deficient bridge structures. The idea here relies on the restrained recovery of shape memory alloys to rehabilitate and strengthen existing bridge structures. Shape memory rods are pre-elongated in the Martensitic phase and then anchored onto the deficient structural system; upon electrical resistance heating and transformation to the

Austenitic phase. The constraints of shape recovery cause corrective (post-tensioning) forces to the structure. It was believed that such approach has the following virtues over conventional approaches: (a) ease and expedience of implementation (electrical resistance heating of shape memory rods can be accomplished using an electrical generator); (b) reduced loss of post-tensioning force because of such effects as slip and elastic deformations (strain far greater than normal elastic strain of steel or composites can be recovered by the shape memory effect); and (c) retention to correct future damages to the structure (damaging effects would elongate the shape memory rods and such elongations could be recovered simply by electrical resistance heating of the rods).

To reduce the cost of unit weight, of smart materials, iron-based shape memory alloys have been developed. Using the iron-based shape memory alloys provides an efficient and convenient means for rapid repair and strengthening of damaged or deficient infrastructure elements. Restraints of shape recovery in these alloys can transfer corrective (post-tensioning) forces to structural systems. The process involves pre-elongation of shape memory rods at ambient temperature, anchorage of pre-elongated rods onto the structural system, and electrical resistance heating (using a common generator) of rods to cause shape recovery and thus apply corrective forces to the structure. Application of the corrective forces by shape memory rods is a versatile approach capable of tackling diverse structural repair and strengthening problems. Laboratory and field tests verified the approach in applications involving repair of flexural and shear damage in reinforced concrete beams.

Smart Prestressing with Shape Memory Alloy *[2]*

It is possible to obtain two-way shape-memory effect by an extensive thermomechanical cycling. This involves heating the alloy above A_f while it is constrained, and subsequent cooling to below M_f, for several cycles. The resulting two-way shape-memory material can undergo large and opposite deformations under heating and cooling for several cycles, and can serve as a two-way actuator. Using this two-way effect, one can apply and remove stress in a structure, which can lead to a smart bridge, where the amount of prestress can be adjusted on an as-needed basis.

This research confirmed the ability of shape-memory wires to transfer stresses to a concrete beam. The magnitudes of these stresses are above the yield stress of the alloy and are well in excess of what is needed to crack the beam. It was found that strands were well bonded by developing mechanical interlock in between the wires. Inadequate concrete cover to the strands caused spalling at the end of the beams. Cracking observed at the end of the beams was verified with acoustic emission source locations. Those experiments demonstrate

the possibility of using this smart material in addition to regular prestressing steel to offset prestress losses after prolonged use or to increase the capacity of an existing bridge.

Superelasticity-based Rehabilitation and Post-tensioning of Bridge Structures *[16]*

Superelasticity has many key attributes such as (1) efficiency and quickness of application; (2) reliable and stable over time under weathering and load effects; (3) damage control under severe load case; (4) capability of self-repairing.

This research relies on the constrained recovery of superelastic and shape-memory alloys for the rehabilitation and strengthening of existing bridge structures and post-tensioning of new prestressed concrete systems. All the work is carried out as follows: Firstly, a suitable alloy composition and processing condition are investigated and chosen. Then, the comprehensive characterization of the superelastic alloy is introduced. In the third step, the structural design procedures are developed. Finally, the experimental verification of the technology is made.

External post-tensioning with superelastic reinforcement to repair and strengthen reinforced or prestressed concrete structural systems was designed in order to increase their service and load capacity their substantial energy absorption and damage control capability.

The cross sectional area, amount of restrain and geometric configuration of the superelastic reinforcement and the end anchorage/adhesion of the reinforcement to the concrete structure are chosen as design parameters. Two design criteria govern post-tensioning with superelastic reinforcement for strengthening and repair: (1) serviceability and strength; and (2) self-repair. The serviceability and strength criterion follows that stress, deflection, crack width and ultimate strength limits have to be satisfied in conventional prestressing. The self-repair criterion in particular, takes advantage of the superelastic phenomenon to build an inherent repair capability into the structure.

B. Some Original Data from Beam Experiments

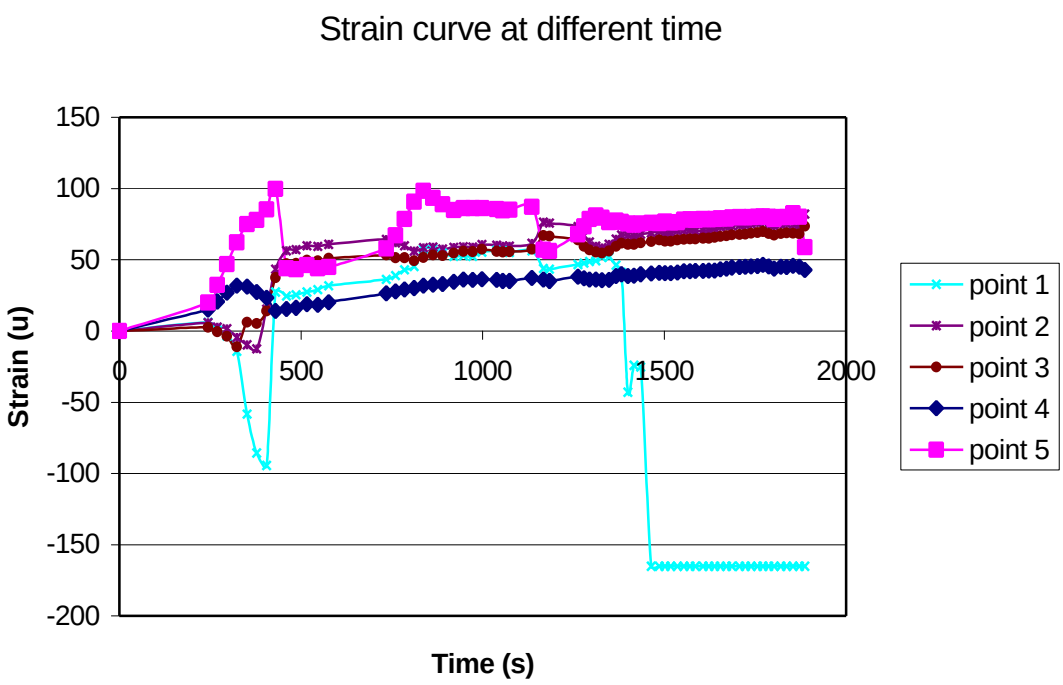

Figure 32
Strain at different times of the second beam

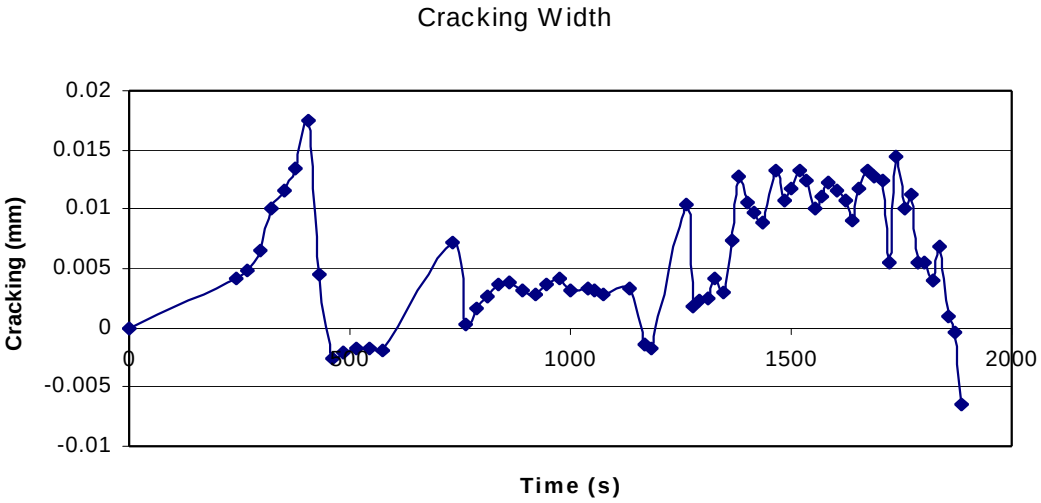

Figure 33
Reading of cracking transducer of the second beam

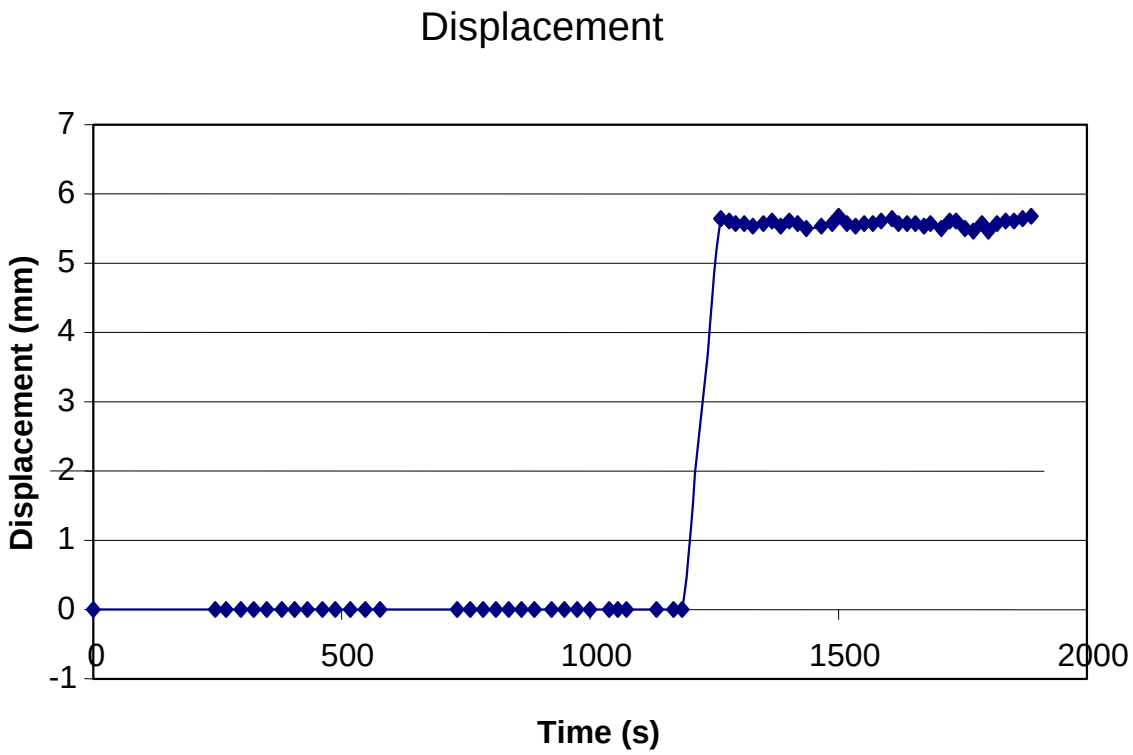

Figure 34
Reading of displacement transducer of the second beam (obvious malfunction of the system)

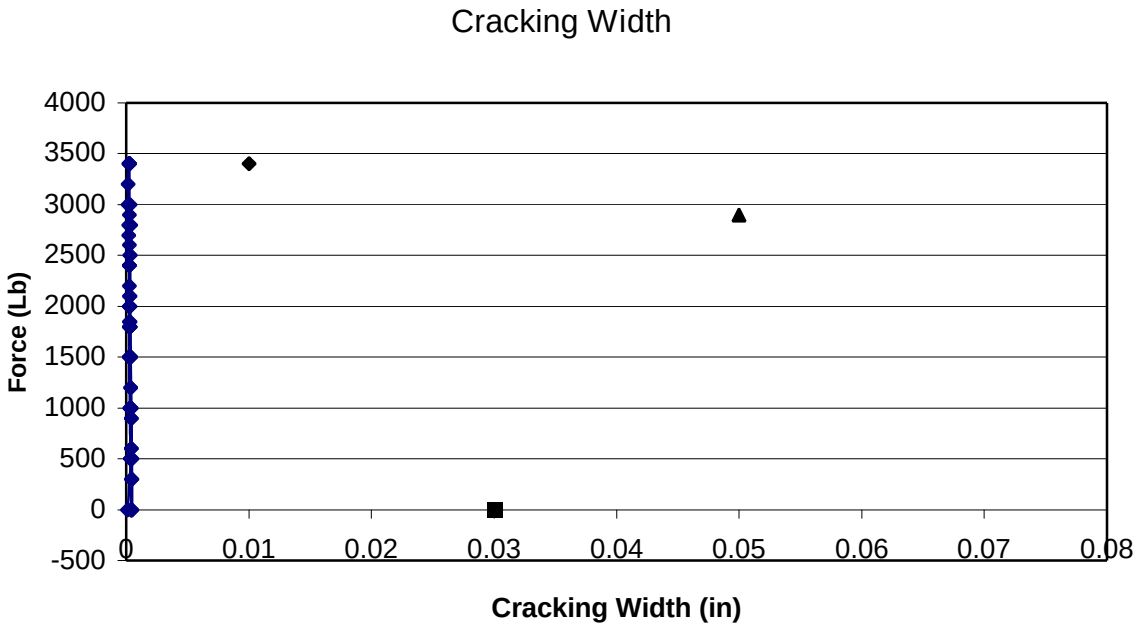

Figure 35
Reading of cracking transducer for the third beam

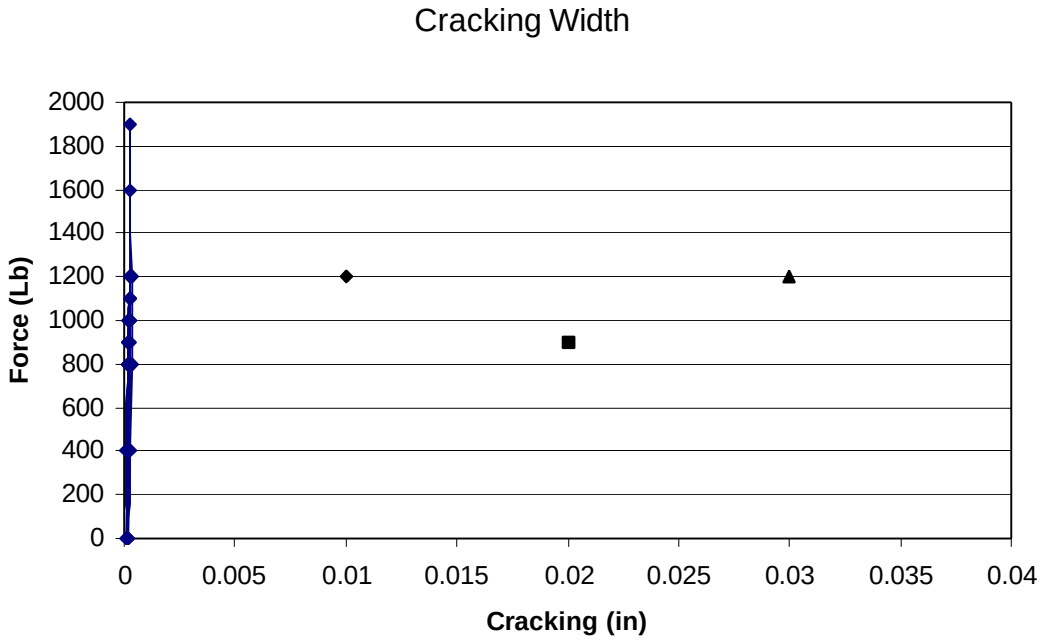

Figure 36
Reading of cracking transducer for the fourth beam

To compare the reading of cracking transducer with the actual cracking width measured with the cracking ruler, we put the actual cracking width (table 8) in figure 35. In this figure, the diamond represents the reading of the second circle, and the triangle and rectangle represent the third circle.

Similarly, we put the actual cracking width in figure 36 for the fourth beam. In this figure, the diamond represents the first circle, the triangle represents the second circle, and the rectangle represents the third circle.